NASA Contractor Report 145374

(NASA-CR-145374) SHUTTLE APPLICATIONS IN TROPOSPHERIC AIR QUALITY OBSERVATIONS Final Report (Mitre Corp.) 122 p HC A06/MF A01 CSCL 13B

N82-11635

Unclas
G3/45 01210

Shuttle Applications in Tropospheric Air Quality Observations

E. Friedman
J. Gupta
J. Carmichael

Metrek Division of The MITRE Corporation
1820 Dolley Madison Blvd.
McLean, Virginia 22102

Contract No.: F 19628-78-C-001
August 1978

National Aeronautics and Space Administration

Langley Research Center
Hampton, Virginia 23665
AC 804 827-3966

NASA Contractor Report 145374

Shuttle Applications in Tropospheric Air Quality Observations

E. Friedman
J. Gupta
J. Carmichael

Metrek Division of The MITRE Corporation
1820 Dolley Madison Blvd.
McLean, Virginia 22102

Contract No.: F 19628-78-C-001
August 1978

NASA
National Aeronautics and Space Administration
Langley Research Center
Hampton, Virginia 23665

ABSTRACT

This study investigates the role which might be played by the Shuttle in obtaining data which describes the air quality of the Eastern United States. A number of aspects of the problem are considered including the data requirements of users, a model for statistical interpretation of the observations, the influence of orbit parameters on the spatial and temporal sampling and an example of application of the model.

TABLE OF CONTENTS

TABLE OF CONTENTS (Concluded)

LIST OF ILLUSTRATIONS

LIST OF ILLUSTRATIONS (Concluded)

LIST OF TABLES

SUMMARY

The purpose of this report is to present the results of a study of the performance of remote sensors of atmospheric pollution when placed in Earth orbit. More specifically, the study addressed the ability of various instrument/orbit combinations to determine pollution levels in the biosphere (herein defined as altitudes from the ground to 2 km) of the Northeastern U.S. This particular area is of interest because of its extensive air pollution and complex inter-urban transport of these pollutants. A considerable national effort is underway to achieve a better understanding of pollution transport and air chemistry of the region. The addition of spacecraft observational capability would add to both studies of historical data (taken at the many air monitoring sites within the region) and data obtained from experiments specifically designed for regional air pollution characterization. Figure 1 illustrates the area of interest.

The National Aeronautics and Space Administration (NASA), sponsor of this study, limited its scope to include specific satellite orbits and remote sensor payloads. The orbits chosen for study were to include those which are consistent with the early missions of the Space Shuttle, on which the proposed experiments might be flown. The sensors chosen for consideration include two of the more advanced atmospheric remote sensors currently under development by NASA.

FIGURE 1
THE AREA OF INTEREST

A typical Shuttle mission appropriate for these experiments might be of seven day duration, have an altitude of 245 km and an inclination with respect to the plane of the equator of 57°. The resulting ground track of the orbit is shown in Figure 2. Based on the choice of orbit parameters, the ground track for this particular orbit will repeat every 111 orbits or, equivalently, after 7 days (hereinafter referred to as the number of days in the repeat cycle of the orbit). Figure 2 also illustrates the area covered by the field of view as it moves along the orbit track.

The sensors selected by NASA as examples in this study are representative of the state-of-the art in passive remote sensing. The selection of specific instruments was related to their state of development and ability to detect carbon monoxide (CO) and other important air pollutants. Carbon monoxide was chosen as the most important indicator of sensor capability because of its importance in the air quality of the Northeastern U.S.

After a review of the possible candidate sensors, two were chosen for review in this study. One of the sensors, MAPS (Measurement of Air Pollution from Satellites), is designed to utilize the infrared radiation emitted by the Earth and its atmosphere to detect trace quantities of carbon monoxide. The principle of MAPS operation is the passage of the atmospheric infrared radiation spectrum through a sample of carbon monoxide in the instrument. The sample selectively absorbs that part of the energy which was emitted by carbon

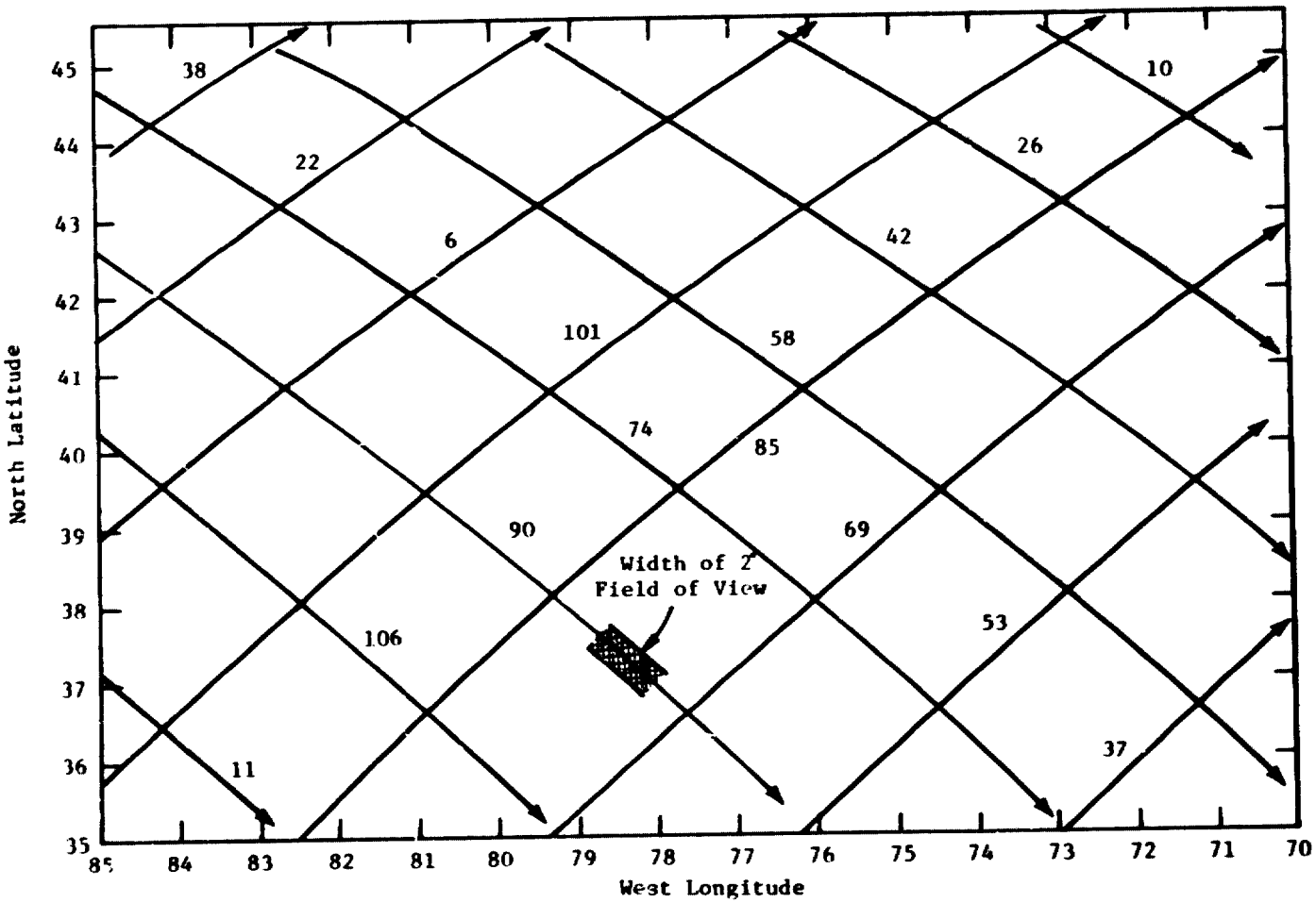

FIGURE 3-5
GROUND TRACK OF TYPICAL SHUTTLE ORBIT (ALTITUDE = 245 km, INCLINATION = 57°). EACH TRACK IS ASSOCIATED WITH THE NUMBER OF ORBITS SINCE THE START OF THE MISSION.

monoxide in the atmosphere, thereby providing a measure of the total amount of that gas within the view of the instrument.

The other sensor, CIMATS (Correlation Interferometer for the Measurement of Atmospheric Trace Species), obtains information on the radiation upwelling from the Earth and its atmosphere in the form of an interferogram (Fourier transform of the radiation spectrum). The interferogram, which covers only a selected portion of the infrared spectrum, is then compared with interferograms recorded under laboratory conditions in order to determine pollution levels. CIMATS is designed to measure the trace gases CO, methane (CH_4), nitrous oxide (N_2 O), ammonia (NH_4) and sulfur dioxide (SO_2).

The MAPS instrument has a nominal full angle field-of-view of 4.33°. CIMATS has a nominal field-of-view of 7°. In both cases the field-of-view can be reducedto about 2° with the aid of a telescope. From a nominal orbit altitude of 400 km, these fields-of-view translate into a 14 km (for 2°) to 50 km (for 7°) resolution element on the surface of the Earth.

The sensors chosen for consideration are somewhat limited in capability as a result of their basic operating principles. A number of these limitations apply to both instruments regardless of the fact that the sensing techniques rely on considerably different concepts and/or parts of the electromagnetic spectrum.

Neither instrument is capable of directly observing the vertical variation in pollution levels. The detected radiation, which is

indicative of the level of pollution, emanates with an efficiency which varies with altitude, each volume element of the atmosphere contributing to some degree. Each measurement, then, is the integral over altitude of the pollution level, weighted by the sensitivity of the instrument to each altitude. The pollution concentration integrated over altitude is called the column burden.

The amount of infrared radiation reaching a sensor in orbit is determined by the simultaneous absorption and emission of radiation by the constituents of the atmosphere. Photons emitted near the ground have a highly variable probability of being absorbed before reaching the sensor, depending on the wavelength and the concentration of atmospheric constituents which absorb at those wavelengths. Photons emitted higher in the atmosphere have a higher probability of reaching the sensor both because the path is shorter and because the density of the atmosphere (and its pollutants) decreases rapidly with altitude. When these effects are translated into graphic form (called a weighting function) as illustrated in Figure 3, it can be seen that infrared instruments are generally insensitive to pollution near the ground and may exhibit maximum sensitivity at altitudes in the 0.5 to 2.5 km range.

The curve illustrates that the altitudes of interest (0-2 km), as well as many others, contribute to the signal detected at the spacecraft. More important, the contribution from the very low altitudes, which are often most polluted, is negligibly small compared to

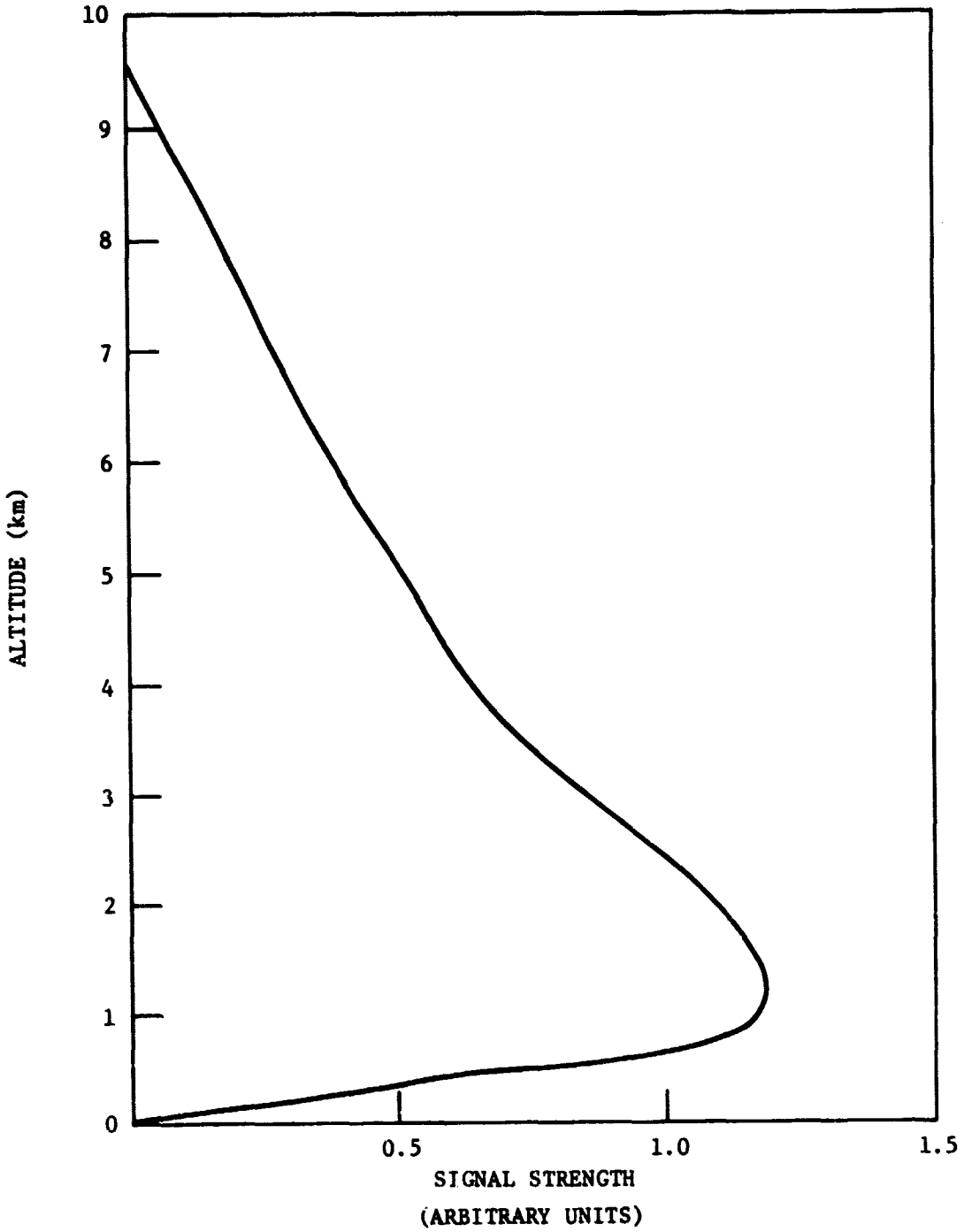

FIGURE 3
WEIGHTING FUNCTION FOR 0.1 ppm CO UNIFORMLY DISTRIBUTED IN THE TROPOSPHERE FOR A LAPSE RATE OF 2 K°/km AND A SURFACE TEMPERATURE OF 298 K.

that of higher altitudes. While the curve is only an example for a particular pollutant at a particular wavelength, it is typical of the sensitivity of infrared instruments.

As an alternative, the CIMATS instrument can utilize reflected solar radiation rather than infrared radiation. In order to have adequate radiation intensity to provide a useful measurement, the solar elevation relative to the point directly below the sensor must exceed approximately 30 degrees. This factor limits the usefulness of CIMATS. Both orbit characteristics and the seasonal variation in solar zenith angle determine the local solar elevation. Figure 4 shows the seasonal variation in elevation of the sun at its zenith for a typical orbit. The figure illustrates that observations are difficult to obtain unless the date of the mission is chosen with care, and also that the length of a mission utilizing CIMATS is limited by solar elevation effects to about 20 days. Measurements derived from CIMATS using solar radiation are also limited in their ability to provide a measure of biospheric pollution. The column burden detected by CIMATS includes a contribution from all altitudes, the weighting function depending on the atmospheric pressure and the relative pollution concentration.

The inability of the instruments to make direct observations of particular altitudes or ranges of altitudes means that pollution levels near the ground, which are of particular interest in this study, can only be obtained after processing of the data. Processing methods

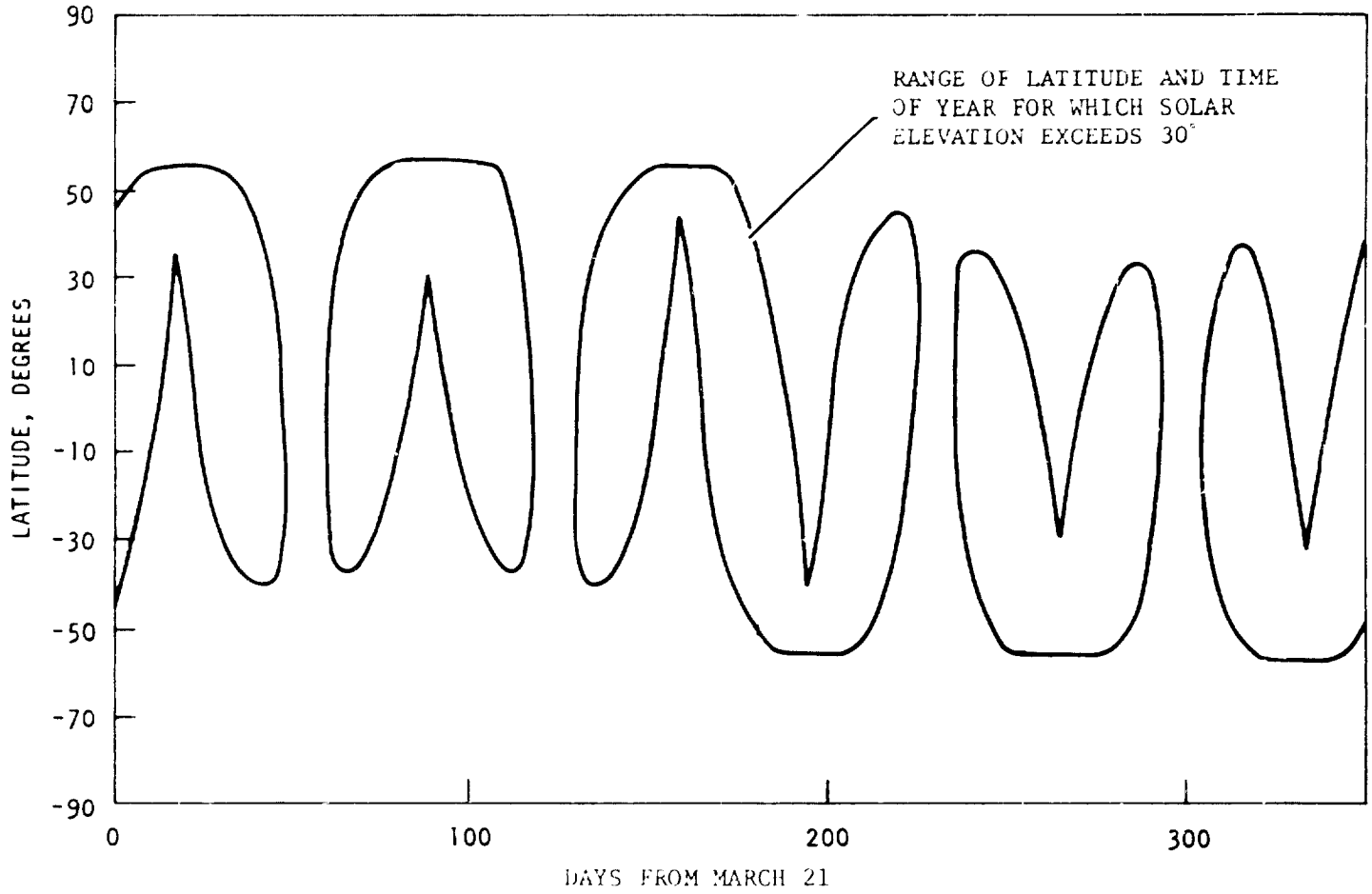

FIGURE 4
LATITUDES COVERED BY A TYPICAL 56° ORBIT WITH THE REQUIREMENT THAT THE SOLAR ELEVATION EXCEEDS 30°

which might provide such estimates of pollution levels have not yet been developed, although it is theoretically possible to obtain such results.

Both instruments would require auxiliary data in order to obtain even column burden information. For example, information on the presence of clouds in the field of view, their location, and altitude are essential since the range of the atmosphere over which the instruments obtain information is interrupted by clouds. Other information necessary for data processing includes temperature and water vapor profiles of the atmosphere.

Yet another limitation of both instruments is that neither has been flown in space. There is doubt about the quality of the column burden data which might be obtained. This lack of flight experience also means that there is no data base which can be used to establish data processing methods which result in the best possible estimates of pollution levels.

In order to quantify the performance which might be expected from various sensor/orbit combinations, a system model was developed during this study. It mathematically describes the potential performance by including sampling characteristics (as defined by orbit parameters and the incidence of cloudiness), instrument factors (such as field-of-view and time constants) and the statistics of pollution variation which are typical for the region of interest. The resulting application of the model is a calculation of the uncertainty

associated with pollution estimates made under various observational conditions. In this context uncertainty refers to an estimate of the measurement error. Direct measurement of the error is not possible in this experiment, since the true value cannot be known, and an *a priori* estimate of the error must suffice. In utilizing the model, it was assumed that appropriate data reduction techniques could be developed so that pollution levels could be detected for the lower altitudes of the atmosphere. Obviously, in the case that such data analysis techniques are not developed, such missions would be of considerably less value. As is commonly the case in remote sensing programs, an effective data analysis procedure is essential.

The sensor/orbit model takes into account the sampling which can be achieved (as determined by orbit conditions and the influence of cloudiness). The sampling is characterized by the spatial distribution of observations over the area of interest as well as the local time of the samples. Temporal sampling is defined by the frequency with which various areas are observed, the local sun time of the observations, and the solar elevation during the observations. Sampling for various orbits was derived from an orbit propagation calculation.

Results of the model appear in Table I where total uncertainties (resulting from all sources) are documented. The Table illustrates the total uncertainty in pollution estimates as a function of mission duration and repeat cycle for a set of pollution statistics derived

TABLE 4-111

TOTAL UNCERTAINTY (IN PERCENT) IN POLLUTION ESTIMATES
ASSUMING 50% CHANCE OF CLOUD COVER AND 50% UNCERTAINTY
IN INDIVIDUAL POLLUTION ESTIMATES

	MISSION DURATION (days)		
REPEAT CYCLE (days)	7	15	30
1	27.9	19.4	13.8
2	37.1	25.5	18.1
3	45.1	30.9	21.8
4	52.6	35.6	25.2
5	56.0	39.8	28.1
6	59.2	43.5	30.8
7	62.3	47.0	33.3

from real data. The analysis includes the effects of incomplete sampling, instrument noise and delays in instrument response to spatial and temporal variations in pollution. The results are presented assuming a 50% uncertainty in individual measurements. This value may vary from instrument to instrument, and the values of Table I may change accordingly. However, the Table clearly illustrates the expected trends, particularly that missions longer than those currently planned are required to obtain the lowest possible uncertainty in pollution measurements. Another important factor is the trade-off which exists between the density of coverage of the area of interest and the data quality. The shorter repeat cycles (which result in the lowest uncertainties) also exhibit the poorest density of sampling of the region of interest. Choosing an orbit which is characterized by a high density of spatial sampling will result in relatively high uncertainty in pollution estimates.

The value of the sensors and missions considered in this study can only be qualitatively judged after comparison with performance needs associated with the regional air pollution problem. Three categories of data uses can be defined, each with its own set of requirements. The first, and most demanding, of these is scientific applications. The data must be of high quality (low uncertainty), exhibit spatial and temporal sampling which allows a complete description of pollution variability in space and time, and have sufficient duration to satisfy the needs of the particular experiment. The second general area of application of the data is monitoring. The

primary needs are that the observational period be very long, the measurements of sufficient quality to determine if standards have been exceeded and the spatial sampling pattern representative (though not necessarily highly dense). Third, public information data needs require only that a general description of pollution location and movement can be made. Missions only need be long enough to describe the movement of pollutants over inter-urban distances. Quantitative concentration data is not essential but the data must supply a general characterization of the problem.

In view of the performance which can be expected from the sensor/orbit combinations under consideration, only the public information role can be satisfactorily performed. Scientific applications require data quality which cannot be achieved by the instrument/orbit combinations, particularly when compared with the capabilities of ground-based sensing systems. Monitoring needs cannot be met because of the rather short duration of the spacecraft missions.

The instrument/orbit combinations do, however, hold the possibility for providing qualitative data on the movement of polluted air masses. Under the conditions imposed by the sponsor on instrument selection and orbit characteristics, this qualitative data will be sufficient to inform the public of the long-range transport of polluted air, illustrate the general relationship between meteorology and air pollution and, possibly, identify major pollution sources. The results of the study also show that mission durations which

greatly exceed the current proposed seven day flight, will result in data quality which, while not being sufficient for scientific or regulatory purposes, may be adequate to provide a reliable picture of pollution levels.

The value of the data to the public will, of course, be a function of its accuracy and the fidelity with which it describes the region of interest. It is evident, then, that data analysis procedures which allow determination of pollution levels near the ground are greatly needed. The experiment as described in this report is arbitarily limited by the fact that only nadir-viewing instruments are considered. The inclusion of some method of cross-track scanning would allow the selection of short repeat cycle orbits (which minimize uncertainty in the pollution estimates) but still provide good spatial coverage of the region of interest by scanning the field-of-view to the areas which the satellite does not fly directly over. This approach is not a complete solution to the spatial-temporal sampling problem, however, since the number of samples is still limited by the duration of the mission. Scanning off the orbit track will reduce the number of observations of areas directly below the spacecraft in order to provide more complete spatial sampling between the orbit tracks. The most appropriate solution to limited sampling is increasing the duration of the mission.

1.0 INTRODUCTION

Providing a clean environment requires that consideration be given to the sources, transport, transformation and sinks of the various pollutants. This is particularly true in the case of the atmosphere, which is a repository for many of man's pollutants (called primary pollutants) as well as being a medium in which chemical and physical changes can occur, resulting in secondary pollutants. The atmosphere has become a sort of chemical factory. During a stay in the atmosphere, various pollutants may undergo photochemical changes, evolve into particles, dissolve in water droplets, become oxidized or reduced, etc. Ultimately, they may find their way into populated areas, create "smog," and cause health effects, material degradation, etc. The complexities and unpredictability of these processes are increased by the fact that the source and the affected area may be far apart due to transport and transformation. The effects are seen in at least two ways; 1) the totality of all sources combine to create a minimum pollution level or "background" which is uniform over large areas (globally in some cases but more commonly over a regional area) and varies slowly with time, 2) a specific source or group of sources produce a plume of pollution whose path can be followed over long distances and which may eventually pollute another area. The distances involved may include the impact of a power plant on areas a few kilometers away to inter-urban transport over a range of hundreds of kilometers. The inter-urban

transport of pollutants is referred to as regional pollution and is the subject of this report. Considerable attention has been given recently to the problem of regional pollution. A survey is included in a recent MITRE Report [1]. The report notes that the conventional observation, modeling and control strategies are less reliable on a regional (inter-urban) scale than when applied to a single urban area, where the scale of the problem is not too large to be dealt with effectively.

Air quality modeling and prediction becomes more difficult since the normal assumptions used in urban air quality models no longer apply:

- Complex and generally unknown conditions exist for the important meteorological conditions of wind, precipitation and atmospheric stability.
- The number of possible fates of the pollutants must be expanded to include deposition on various surfaces (lakes, rivers, forests, etc.), washout in rainfall or snowfall and chemical or physical transformations which normally cannot occur in the time scale of pollution transport across an urban area.
- Typical diurnal variations in wind, temperature and atmospheric turbulence are different for urban and rural areas. Daily (diurnal) variations in wind or atmospheric turbulence must be considered. Other atmospheric conditions also exhibit variations between urban and rural areas making their influence on pollution chemistry difficult to assess.
- Natural sources of air pollution may be of significance at the scale of space and time characteristic of regional air pollution.

Control of air pollution produced in another city, state or region of the United States clearly invites the participation of

regional or Federal authorities. They are faced with the difficulty, however, that the complex transformations which may occur over some indeterminate route produce secondary pollutants whose source cannot be identified. This problem can be resolved to a great extent, of course, by observational programs which follow the "plume" of an urban area or industrial complex, monitoring the chemical and physical transformations which may occur in its many pollutants, and determine those localities where the pollution has an impact on air quality. Even pollutants emitted from tall stacks, as is common for power plants, may have a distant effect through mixing in the atmosphere, settling (in the case of particulates) or changes in vertical components of the wind. A number of studies of these problems have been carried out and are cited in reference [1].

There are clear limitations, of course, in the ability of an observational effort to produce an adequate characterization of the processes which result in pollution remote from the source. A proper experiment would have to include: continuous monitoring over the entire area of interest, monitoring of vertical and horizontal variations in space and time of all pollutants and their possible derivatives, and determination of factors which control chemical conversion including catalytic materials, meteorological conditions, solar intensity, etc. Even the most ambitious effort cannot collect all of this data on a continuous basis, particularly if conventional ground-based sensing systems are used alone. For this reason, most

recent regional air pollution studies have included at least some airborne sensing for improved spatial coverage although these airborne sensing systems commonly use the same instruments as used in ground-based observations. These instruments are either "contact sensors", which rely on moving a gas sample through a chemical or optical sensing system or "grab samples" which require that a gas sample be obtained, stored and brought to a laboratory device for analysis. Experiments of this type are limited in their duration either because of periods of bad weather, instrument maintenance, or more commonly, lack of funds for aircraft, personnel, and processing of large quantities of data. They do provide advantages over ground-based sensor systems since three dimensions of pollution variation can be detected and large areas can be quickly covered with each set of sensors.

Another approach to regional air pollution studies is the use of historical data assembled from selected ground-based observation stations distributed over the entire region. These stations are usually in place as part of the air monitoring program of a particular city or state and have been independently calibrated so that their data may not be entirely consistent. They do provide however, a record of pollution levels over long periods of time, something not provided by most regional experiments. There may also be considerable limitation in the type of primary and secondary pollutants which are sampled. For example, a community may want to monitor sulfur dioxide (SO_2) to determine if it meets state or Federal standards,

with little concern for the sulfate aerosols which evolve from SO_2 (since that transformation may occur many kilometers away, many hours later). However, that same community may be polluted by sulfates which began as SO_2 far away at an earlier time. A complete experimental program would attempt to monitor both the upwind and downwind SO_2 and sulfates and the rate of transformation of SO_2 to sulfate in space and time. Clearly each approach to regional air pollution studies is limited and invites improvement, basically in the area of spatial and temporal sampling.

This study is designed to provide consideration of yet another means of contributing to both historical studies and specific experiments by making use of remote sensing techniques. Airborne remote sensing has been utilized in some regional experiments but is relatively uncommon (contact sampling or grab sampling for laboratory analysis is much more common). Satellite remote sensing has supported such experiments by providing information on clouds, wind fields, snow and ice cover, etc. The remote sensing techniques discussed in this report can potentially provide information on pollution concentrations by making use of the radiation upwelling from the atmosphere and the surface of the Earth (both infrared and visible wavelengths can be used). The detection is performed by spectroscopic analysis of the radiation and can provide data on the fraction of the atmosphere which is made up of specific pollutant gases. The principles of operation for each instrument are discussed

in Section 2, along with data on the gases which can be detected, sensitivity, etc. The spatial and temporal sampling which can be achieved in applying these instruments will be a function of the satellite orbits used. Section 3 provides a discussion of the spatial and temporal sampling which can be expected, with specific reference to an area of the U.S. which is commonly affected by inter-urban transport of air pollutants, the Northeast.

Characterization of the data quality which can be expected from the instrument/orbit combinations results from a statistical data interpretation model, described in Section 4. It describes the uncertainty associated with estimates of the pollution as a result of three contributing factors:

- uncertainties associated with incomplete spatial and temporal sampling
- uncertainties in individual pollution estimates associated with random and bias instrument errors
- uncertainties associated with the response of the instruments to the spatial and temporal variability in the natural pollution concentration

Section 5 discusses the data needs associated with various types of regional air pollution studies. Three possible applications are considered: 1) scientific studies intended to improve our understanding of the physical and chemical processes involved in regional air pollution, 2) monitoring studies intended to better characterize the sources, transformation and fate of air pollutants and 3) public

information of the data as a tool in raising the public's awareness of the long range impact of air pollutants.

Section 6 presents a comparison of the data needs of Section 5 and the expected data quality as derived in Section 4.

REFERENCE

1. E. L. Keitz, E. J. Friedman and R. G. Eldridge, "The Capability of Remote Sensing for Regional Atmospheric Pollution Studies," MITRE Technical Report MTR-7267, January 1977.

2.0 INSTRUMENT PERFORMANCE

The acquisition of meaningful air quality data will require that the instruments chosen for the missions can detect the appropriate gases, have relatively low noise and sensitivity to interfering species, and can differentiate the low altitude component of the column burden. It is the intent of this section to characterize the anticipated operating capability of the sensors under consideration (CIMATS and MAPS)* as well as discuss their ability to provide data on the pollution of the biosphere. This information will be used in Section 4 as input to the system performance model.

2.1 General

Over the past several years many instruments have been developed for remote sensing from satellite platforms. Previous reports have treated these sensors and their operating characteristics in great detail [1,2]. Given the interest in carbon monoxide as an urban and regional pollutant and the relative state of development of the various sensors suitable for space missions, the choice of instruments to consider for the purposes of this report was considerably narrowed. Only MAPS and CIMATS will be treated in this study as they are, at present, the only passive instruments with a designed capability for the measurement of CO. Each has also had sufficient field testing to allow some degree of confidence about the performance which might be expected.

*Correlation Interferometer for the Measurement of Atmospheric Trace Species; Measurement of Air Pollution from Satellites

2.2 MAPS

The MAPS instrument uses gas filter correlation in order to obtain high radiation throughput and resolution. A sample of the gas of interest, say CO, is placed in a gas cell located in an optical path carrying radiation from the scene to the detector. Another, otherwise identical, path traverses an evacuated cell. The difference in the electrical outputs of the detectors is the signal difference which provides an indication of the amount of the gas of interest between the infrared radiation source (normally the Earth and its atmosphere) and the instrument. A further refinement in the MAPS instrument involves the inclusion of a gas cell at a different partial pressure of the gas of interest than is contained in the first gas cell. By comparing the difference signals derived from each gas cell and the evacuated cell, the measurement is less subject to errors caused by the presence of interfering species in the atmosphere [3]. An added potential advantage in the use of two gas cells of different pressures is the ability to obtain some coarse information on several vertical layers of the atmospheric path.

Figure 2-1 shows the optical layout of the MAPS instrument. The reference blackbody is sampled alternately with the scene radiation to provide a baseline reference level. The hot and cold blackbodies are adjusted to span the anticipated temperature range of the scene. They are sampled at a higher frequency than the scene energy and reference blackbody in order to allow electronic separation of

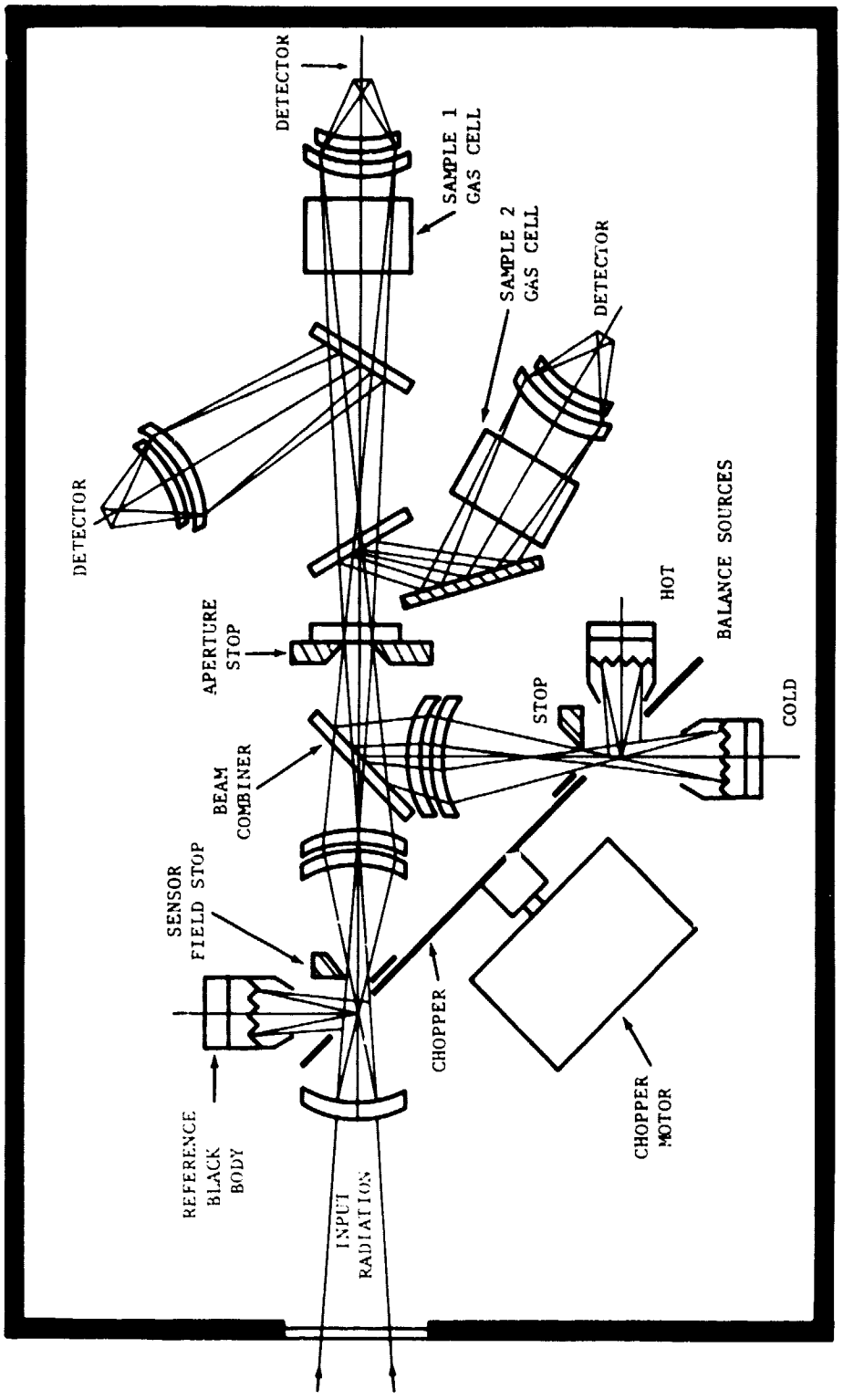

FIGURE 2-1
MAPS OPTICAL LAYOUT[5]

the signals for subsequent processing. Gain controls on the electronics are driven by the balance sources so as to keep the gain of the gas cell paths equal to that of the vacuum path for both temperature extremes. This procedure effectively balances the system and reduces the effects of variations of radiance reaching the two detectors [4]. For the optical path through the evacuated cell, the modulated energy from the balance sources is used for radiometric calibration, while that from the scene and reference is used to determine scene brightness.

The MAPS instrument is scheduled to fly on a Shuttle mission in 1979. Table 2-1 shows the instrument characteristics which will be used for that experiment. In recent aircraft tests, the two gas cells have been filled with CO at partial pressures of 0.35 atmospheres and 0.1 atmospheres. Current efforts are directed at determining the optimum pressures for these two cells.

In the nadir-viewing (or vertically down-looking) mode, MAPS will provide data on the total column burden of CO in cloud-free areas of the Earth. Planned refinements in the choice of gas partial pressures and data processing may result in data representative of two broad vertical bands in the atmosphere. The importance of these developments is discussed in Section 2.4.

2.3 CIMATS

The CIMATS instrument is a two channel infrared (IR) interferometer which uses the same general principles of operation as its predecessor,

TABLE 2-I

MAPS EXPERIMENT CHARACTERISTICS [6]

Field-of-view, degrees	4.33
Spectral range, micrometers (μm)	4.5-4.8
Aperture, centimeters	2.94 x 2.94
Sensitivity, (NEN), watts/ steradian-centimeter^2	1.7×10^{-8}
Detectors (3)	PbSe
Detector temperature, degrees kelvin	195
Detector cooling	Thermoelectric
Response time, seconds	8 to 10
Data sampling interval, seconds	
Signal channels	1.0
Temperatures	15
Data storage, bits per second (self-contained tape recorder)	50
Input power, watts	2814
Standby	80
Balance/Calibrate	95
Operate	105
Size, including single baseplate, cm	75 x 75 x 45
Weight, kilograms	65

the COPE* instrument [7,8,9]. The A channel uses reflected solar energy in the near-IR (2-2.4 μm) and the B channel uses thermal radiation of the Earth and its atmosphere (4-9 m). Table 2-II indicates the various species for which CIMATS is currently being built and the filter parameters associated with each measurement. The A channel will use lead sulfide (PbS) detectors cooled to 195°K with a noise equivalent power (NEP) of 5×10^{-13} watts per root hertz ($w/\sqrt{Hz}$). The B channel uses mercury - cadmium - telluride (HgCdTe) detectors, cooled to 77°K by liquid nitrogen, having a NEP of 3.5×10^{-11} $w/\sqrt{Hz}$ at 8.9 m. The instrument field-of-view is nominally 7° with a 2° field-of-view option when a second telescope objective is used.

The instrument is a variant of a normal Michelson interferometer. A time-varying path difference is introduced into one of the optical paths by the rotation of a phase plate. The other optical path is of constant length (phase). Recombination of the two paths results in an alternating reinforcement and cancellation, depending upon the phase difference of the two rays. The result is analogous to a Fourier transform of the incident radiation. The effect of this design is to transform the electromagnetic variation at optical frequencies to electrical signals which can be conveniently processed. The basic components of the instrument are illustrated in Figure 2-2. The range of scan (phase delay) is chosen to optimize the signal-to-noise ratio for a particular species of pollutant in the atmosphere.

*Carbon Monoxide (CO) Pollution Experiment.

TABLE 2-II

CIMATS OPTICAL PARAMETERS [10]

Channel	Species Measured	Center Wavelength	Filter Width
A	CO, CH_4	2.33 $\pm$ 0.005 μm	0.0008 μm
A	N_2O	2.26 $\pm$ 0.005 μm	0.0008 μm
A	NH_3	2.23 $\pm$ 0.005 μm	0.0007 μm
B	CO, N_2O	4.62 $\pm$ 0.021 μm	0.0968 μm
B	SO_2	8.70 $\pm$ 0.038 μm	0.0529 μm

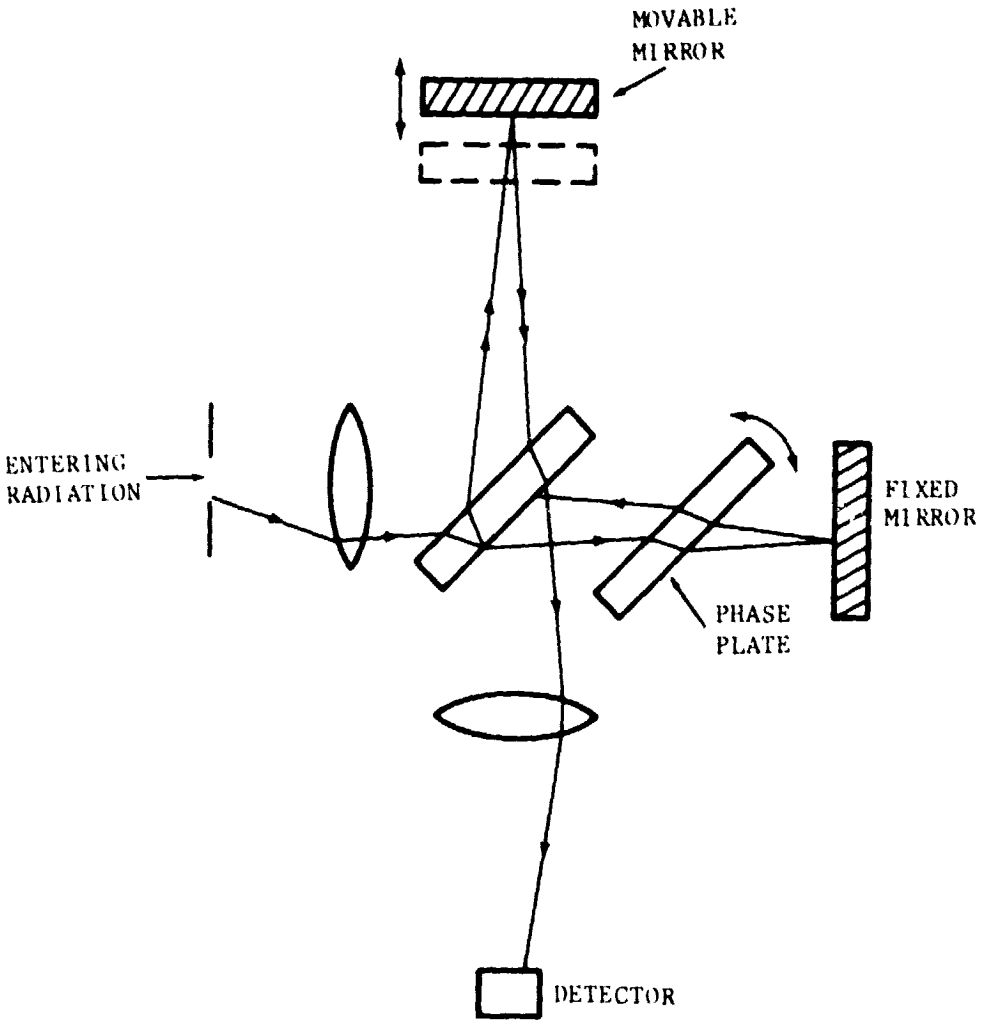

FIGURE 2-2
THE CIMATS INTERFEROMETER [6]

In the presence of interfering species, the interferogram does not provide a unique indication of the species of interest. Table 2-III lists the major interferent and the expected signal-to-noise ratio for each measurable species. To reduce interference effects, use must be made of weighting functions which are chosen to minimize the contribution made by constituents other than those of interest, while maximizing the signal-to-noise ratio of the desired species. The weighting functions are determined both theoretically and experimentally. The best available atmospheric models and spectral absorption properties are used to construct a "base interferogram." Variation of the concentrations of various constituents results in a set of different interferograms. Since each interferogram consists of a set of data points, the set of interferograms may be considered a set of simultaneous linear equations which, in turn, may be solved for the appropriate weighting functions. Laboratory experiments are then performed to generate interferograms based upon actual gas concentrations at a range of partial pressures.

In operation, interference filters limit the range of the radiation incoming to the instrument to a very narrow band, selected to coincide with the region where the effects of absorption by the species of interest are greatest. Interferograms are generated while observing the area of interest in a nadir-viewing (vertical down-looking) mode, one complete scan requiring 1 to 3 seconds. These interferograms are compared to the stored weighting functions to determine

TABLE 2-III

INTERFERANTS AND ANTICIPATED SIGNAL-TO-NOISE RATIOS [S/N] FOR CIMATS MEASUREMENTS [10]

Channel	Species	Assumed Background	Center Wavelength	Interferants	S/N
A	CO	0.1 ppm	2.33 μm	CH_4, H_2O	20:1
A	CH_4	1.5 ppm	2.33 μm	CO_2, H_2O	40:1
A	N_2O	0.2 ppm	2.27 μm	CH_4, NH_3	10:1
				CO_2, H_2O	
A	NH_3	1.0 ppb	2.23 μm	CH_4, H_2O	2:1
B*	CO	0.1 ppm	4.62 μm	CO_2, H_2O	2:1
B*	N_2O	0.2 ppm	4.62 μm	CO_2, H_2O	2:1
B*	SO_2	2.0 ppb	8.70 μm	CH_4, N_2O	not available
				O_3, H_2O	

*S/N ratios of thermal channel are based on the assumption of no independent measurement of temperature profile of the atmosphere. Availability of such measurements will increase S/N ratios.

the best fit of the data. Scale factors may be applied to the weighting functions in order to facilitate this matching process. When the correct weighting function is applied to the data, the result gives the column burden of the specie of interest. In some cases, CIMATS will require vertical profiles of temperature, pressure and humidity to perform calibrations.

2.4 Current Limitations of the Instruments

Both MAPS and COPE have been used for the measurement of the column burden of CO from aircraft platforms but neither has yet been flown on spacecraft. MAPS is tentatively scheduled for inclusion on Orbital Flight Test (OFT) 2 of the Space Shuttle in July 1979. No data base, therefore, exists which could serve to indicate the accuracies of these instruments when used on a satellite. Based upon the experience of each instrument at aircraft altitudes, there is little doubt that each can obtain measurements which are related to the total column burden of the gas of interest.

For the purposes of measuring air pollution as it affects the biosphere, however, column burdens may not be sufficient. As a minimum, the concentrations of various pollutants within the biosphere will be required, and for the purposes of public health, concentrations at lower altitudes will be of greater importance. The ability of the instruments to measure pollution levels at low altitudes depends on their operating characteristics. For example, the use of infrared radiation emitted by the Earth and its atmosphere results in

a vertical sensitivity or "weighting function" as shown in Figure 2-3. The maximum sensitivity occurs for altitudes ranging from 0.5 to 2.5 km, but the instrument is insensitive to pollution very near the ground because the gas temperatures are nearly equal to the ground temperature. The shape of the curve results from the fact that the amount of infrared radiation reaching the sensor in orbit is determined by simultaneous absorption and re-emission by the constituents of the atmosphere, particularly the pollutant gas. Radiation emitted near the surface of the Earth has a relatively low probability of reaching the sensor without first being absorbed, since the radiation for which the sensor is tuned is, by definition, that part spectrum which is characteristic of the gas of interest. The radiation emitted from higher altitudes has increased probability of reaching the detector, both because it traverses a shorter distance and because the influence of the pollutant gas may be reduced for two reasons: 1) its fraction of the atmosphere may be declining because it is concentrated near the ground, and 2) the density of the atmosphere as a whole decreases with altitude. The result of these effects results in a curve typified by Figure 2-3 (if the assumptions indicated in the figure caption apply). The signal produced by the sensor will be a sum of the signal levels contributed by each layer of the atmosphere. Because the actual conditions of the atmosphere during the observations are not known, the sensor signal cannot directly give information on the pollution level of the near-ground region. Use of solar

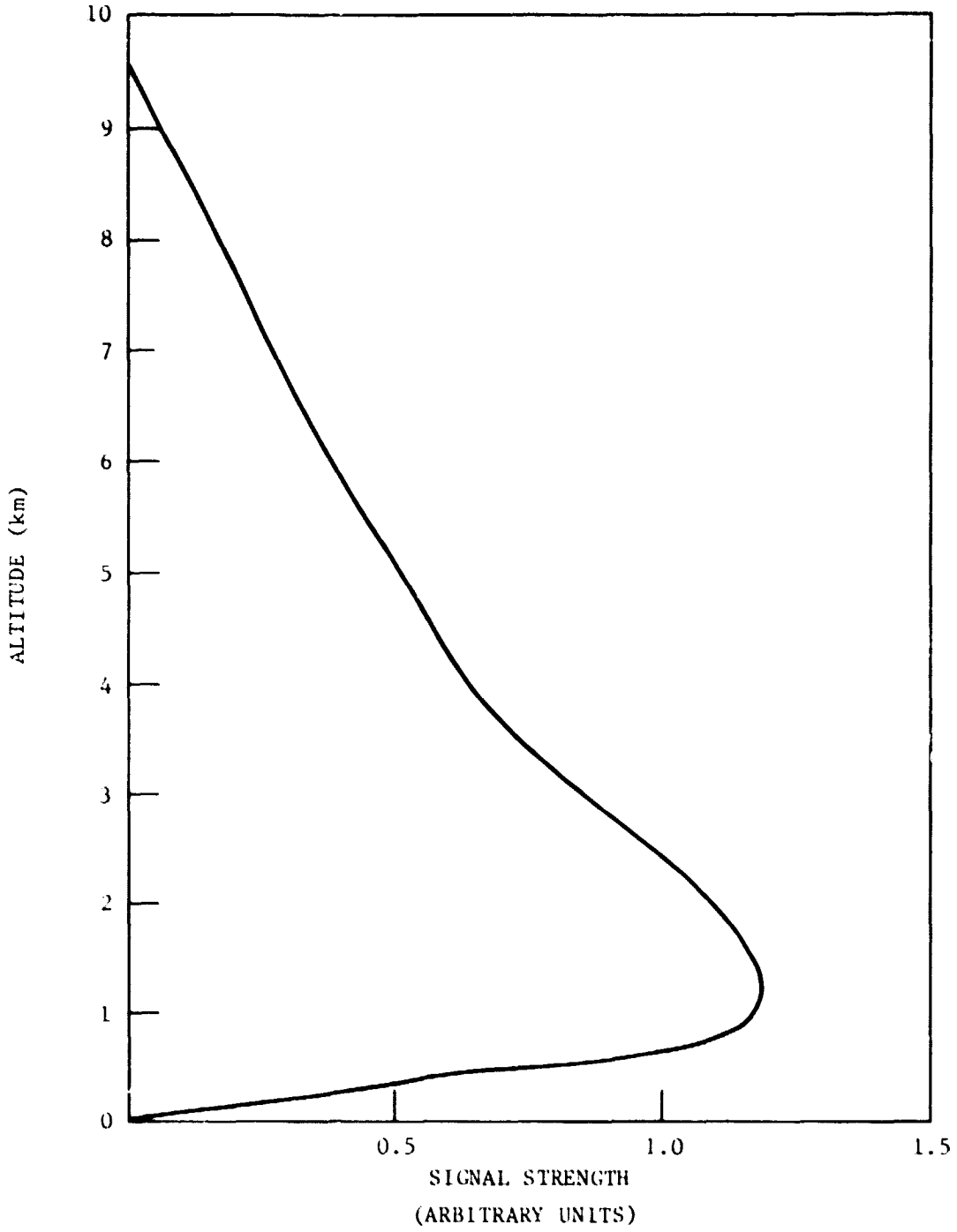

FIGURE 2-3
WEIGHTING FUNCTION FOR 0.1 ppm CO UNIFORMLY DISTRIBUTED IN THE TROPOSPHERE FOR A LAPSE RATE OF 2 K°/km AND A SURFACE TEMPERATURE OF 298 K.[11]

radiation, as can be done with CIMATS, also results in a signal which is not totally representative of the pollution level near the ground. The radiation reaching the sensor has passed through the atmosphere to the ground, back through the atmosphere to the sensor being absorbed by the pollutant(s) of interest along the way. Because the rate of absorption per meter along the radiation path is determined by the number of pollutant molecules, absorption of radiation is a function of both the atmospheric pressure and the relative pollution concentration. Again, these conditions are not known in general so that special data processing techniques will have to be developed to provide near-ground estimates.

While no claims are presently made that either instrument can obtain vertical profiles of pollutants, it may be useful to consider the possible methods which could be used to extract some vertical information from either MAPS or CIMATS.

For both MAPS and CIMATS, clouds pose a problem in coverage. For reflected solar radiation, they, rather than the Earth, provide the reflecting target. For emitted thermal radiation, clouds appear opaque and form the lowest altitude from which radiation reaches the instrument. It might be possible to convert this apparent liability into an advantage. It is possible to obtain some information on the concentration of pollutants in the layer between the Earth's surface and the cloud cover by taking the difference in signals between scenes of complete cloudiness and complete lack of clouds.

In order for this system to be useful, some auxilary information would be required. One would have to know cloud locations within the field-of-view. Cloud heights, temperatures and extents would also be required to effectively analyze the data. This technique is, of course, limited by the meteorology which happens to occur at the time of the overflight and is, therefore, unpredictable. The use of a scanning small field-of-view instrument would help in this regard since the instrument could be oriented to the clear or cloudy regions in a scene.

For MAPS, another possibility for vertical information of gas concentration may be found in the partial pressures with which the gas cells are filled. Since the gas cells provide the filter against which the incoming radiation is compared, the pressures of the cells can be selected to correspond to the pressure of the atmosphere at a particular altitude of interest. Work currently underway on the instrument would provide peak responses in the 600 millibar (mb) and 200 millibar (mb) ranges, which correspond to altitudes of 4 km and 12 km. While these altitudes are not particularly appropriate to the current need (0 - 2 km), the possibility remains that estimates for lower altitudes could be made by interpreting data obtained with weighting function peaks at several altitudes.

CIMATS potentially allows for two other methods of extracting vertical information. The first involves the use of the thermal (infrared) channel and auxiliary data on the atmospheric temperature

and water vapor profiles. This collection of data allows modeling of the radiative transfer of the atmosphere, and estimation of the vertical profile of pollution. The accuracy of the estimates will be a very strong function of the accuracy of the temperature and water vapor profile data. The second method applicable to CIMATS would be to observe the same pollutant simultaneously in both the solar and thermal channels (A and B channels). The solar channel observes the total column of the atmosphere from the ground (or cloud tops) to the sensor as well as the path from the ground toward the sun. The radiation received by the thermal channel will be mainly from the altitude to which the instrument is most sensitive (as typified by Figure 2-3). Suitable processing of this data could yield information on the appropriate altitude range.

The thermal channels of CIMATS and the MAPS instrument might also be able to achieve measures of near-ground pollution by processing the noise in the scene. The signal which reaches the instrument is made up of radiation from the atmosphere within the field-of-view of the sensor (the so-called path radiance) along with a contribution from the ground. Generally, the time variation in the atmospheric signal is small since transport and diffusion tend to make the atmosphere uniform over a relatively large scale. The ground signal, however, may vary considerably in time due to the nonuniform emissivity of the various components of the surface (land, water, vegetation, etc.). So, by preferentially detecting the

rapidly varying component of the signal, one can be sure that it has been produced by radiation from the ground. This method has been developed for a commercially available remote sensor [12].

None of the many data processing concepts mentioned in this subsection has been successfully used to achieve accurate estimates of tropospheric air quality from space. Considerable work would be required to establish the most appropriate methods. The use of thermal radiation as a source for the sensors requires the simultaneous provision of auxiliary data, particularly water vapor and temperature profiles. In addition, information must be available on the extent of cloudiness, the distribution of cloudiness within the scene and cloud top temperature. Generally, the quality of the data produced by the sensor will depend upon the quality of the support data.

Sulfur dioxide and oxidants are particularly important components of regional air pollution. Detection of SO_2 by both sensors is limited by a smaller than acceptable signal to noise ratio. Detection of other important pollutant gases (oxidants, hydrocarbons, etc.) are not claimed for either instrument.

A product of the chemistry of sulfur dioxide and nitrogen dioxide in their regional transport is a variety of aerosols (both sulfates and nitrates). Neither instrument under consideration has been designed to detect these products of stationary source pollution.

A last point of concern is the inability of the solar channels of CIMATS to perform effectively except under appropriate solar

elevation conditions. Figure 2-4 illustrates the yearly variation of latitudinal coverage which can be achieved from a 56° orbit if 30° solar elevation is required. The Figure shows limitations in the use of CIMATS for various times of the year and also illustrates that missions greater than about 20 days are not possible. During that period, the motion of the orbit plane relative to the Earth-sun line causes considerable changes in the solar elevation along the ground track of the orbit. Use of the solar channel of CIMATS in the Northern Hemisphere in winter is also precluded above latitudes of about 30°.

In summary, then, the sensors exhibit considerable development in their concept and design but appear to be limited in performance, particularly from the point of view of obtaining pollution estimates in the highly polluted part of the atmosphere near the ground.

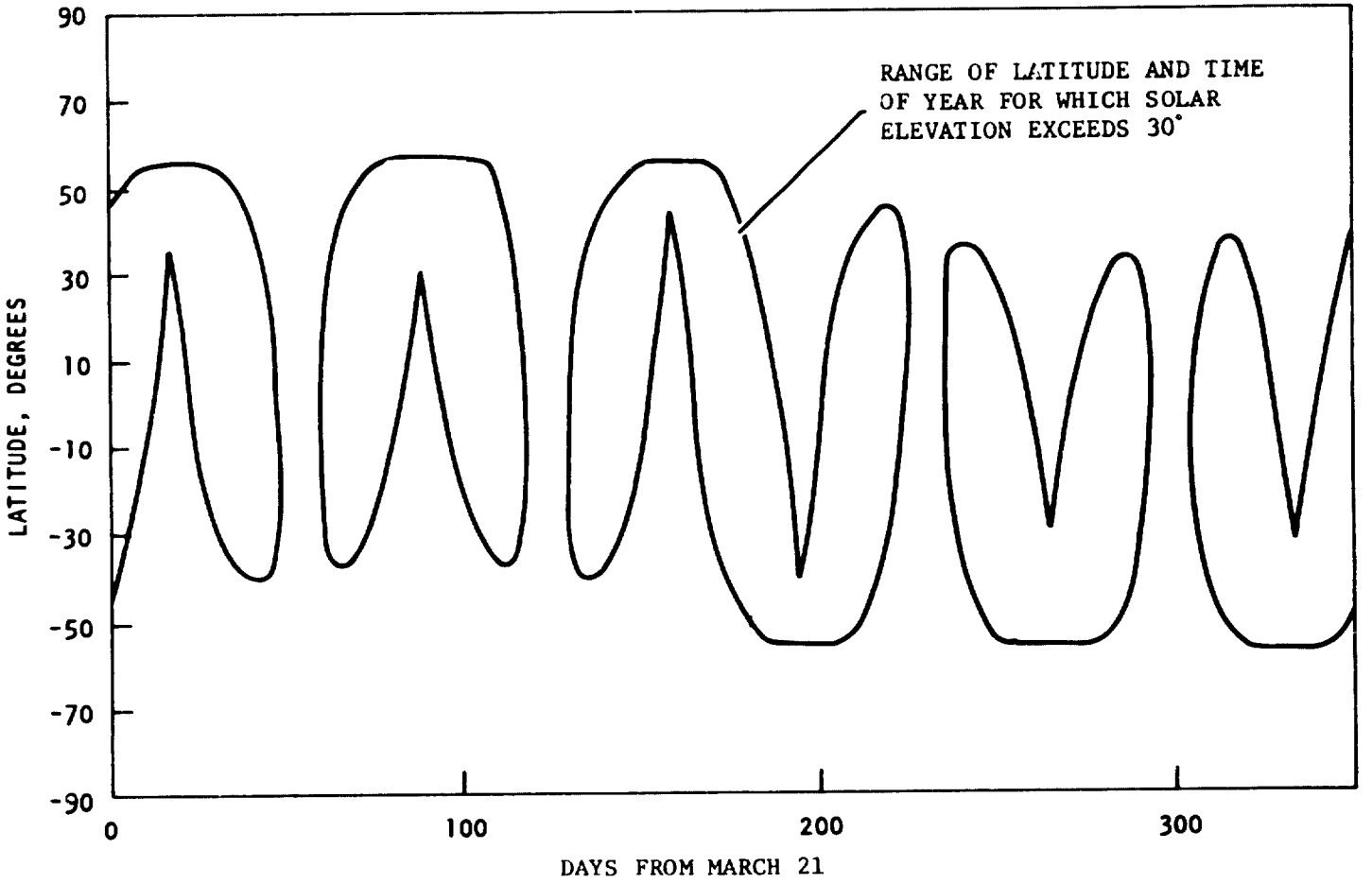

FIGURE 2-4
LATITUDES COVERED BY A TYPICAL 56° ORBIT WITH THE REQUIREMENT THAT THE SOLAR ELEVATION EXCEEDS 30°

REFERENCES

1. L. J. Duncan et al., "An Airborne Remote Sensing System for Urban Air Quality," MITRE Technical Report MTR-6601, February 1974.

2. J. J. Carmichael et al., "Evaluation of Satellites and Remote Sensors for Atmospheric Pollution Measurements," MITRE Technical Report MTR-7170, NASA Report CR-144870, September 1976.

3. TRW, Inc., "Monitoring Air Pollution from Satellites (MAPS)," NASA CR-145137, Final Report, 1 March 1977.

4. T. V. Ward and H. H. Zwick, "Gas Cell Correlation Spectrometer: GASPEC," Applied Optics, XIV, pp. 2896, December 1975.

5. W. D. Hesketh, et al., "A Gas Filter Correlation Instrument for Atmospheric Trace Constituent Monitoring," Proceedings of the Fifth Annual Remote Sensing of Earth Resources Conference, Tullahoma, Tennessee, March 19-30, 1976.

6. S. Beck, NASA, Langley Research Center, private communication, July 1977.

7. M. H. Bortner, et al., "Analysis of the Feasibility of an Experiment to Measure Carbon Dioxide in the Atmosphere," NASA CR-2303, October 1973.

8. R. Dick, et al., "Development of an Engineering Model Correlation Interferometer for the Carbon Monoxide Pollution Experiment," General Electric Company, Philadelphia, Pennsylvania, November 1974.

9. M. H. Bortner, et al., "Carbon Monoxide Pollution Experiment: Final Report," NASA CR-132717, January 1975.

10. P. LeBel, NASA, Langley Research Center, private communication, June 7, 1977.

11. H. G. Reichle, "Measurement of Air Pollution from Satellites." Langley Research Center, NASA, April 1973.

12. _____, "The Ground Chopping GASPEC I," News item in the 1973 Industrial Research Product Annual, p. 37.

3.0 ORBITS

The characteristics of the orbit(s) chosen for the mission will exhibit a considerable influence on data quality. The altitude is directly related to the spatial resolution of the observations and determines, along with the orbit inclination, the spatial and temporal coverage and sampling. Orbit parameters, along with the launch date, control the solar elevation along the orbit track which is important for the proper operation of CIMATS in its visible light mode. The orbit parameters also determine the repeat cycle of the orbit, expressed as the number of orbits (or equivalently the number of days) between ground tracks which exactly coincide. The repeat cycle controls the frequency with which observations are made of a particular site.

The orbits which might be expected for Shuttle missions will range from approximately 250 to 450 kilometers in altitude and from 28.5 to 57 degrees in inclination. Appropriate selection of values from each of these ranges will result in orbits whose repeat cycles are an integral numbers of days. (The more general case is that the repeat cycle will not be an integral number of days). Examples of such orbits are shown in Figures 3-1 through 3-5 and Table 3-1. The figures illustrate the ground track which will occur for 1,2,3,4, and 7 day repeat cycles. Each set of ground tracks will repeat after the number of days in the orbit's repeat cycle.

The orbits shown as examples illustrate that as the length of the repeat cycle gets longer, the density of ground tracks increases. At the same time the frequency of observation decreases.

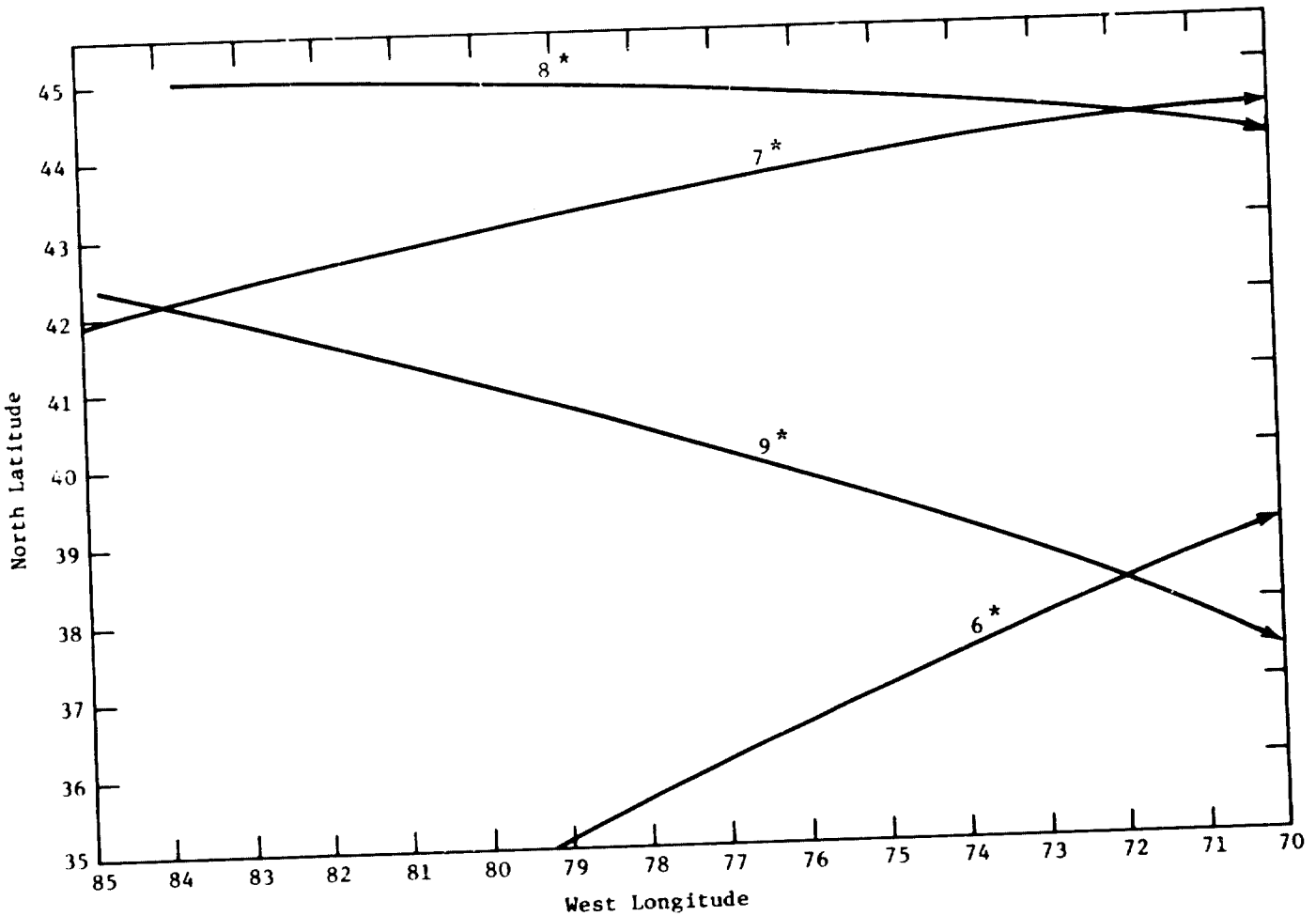

* Indicate which orbit of the cycle is responsible for each ground track.

FIGURE 3-1
GROUND TRACK FOR ORBIT WITH ONE-DAY REPEAT CYCLE
(altitude = 492 km, inclination = 45°)

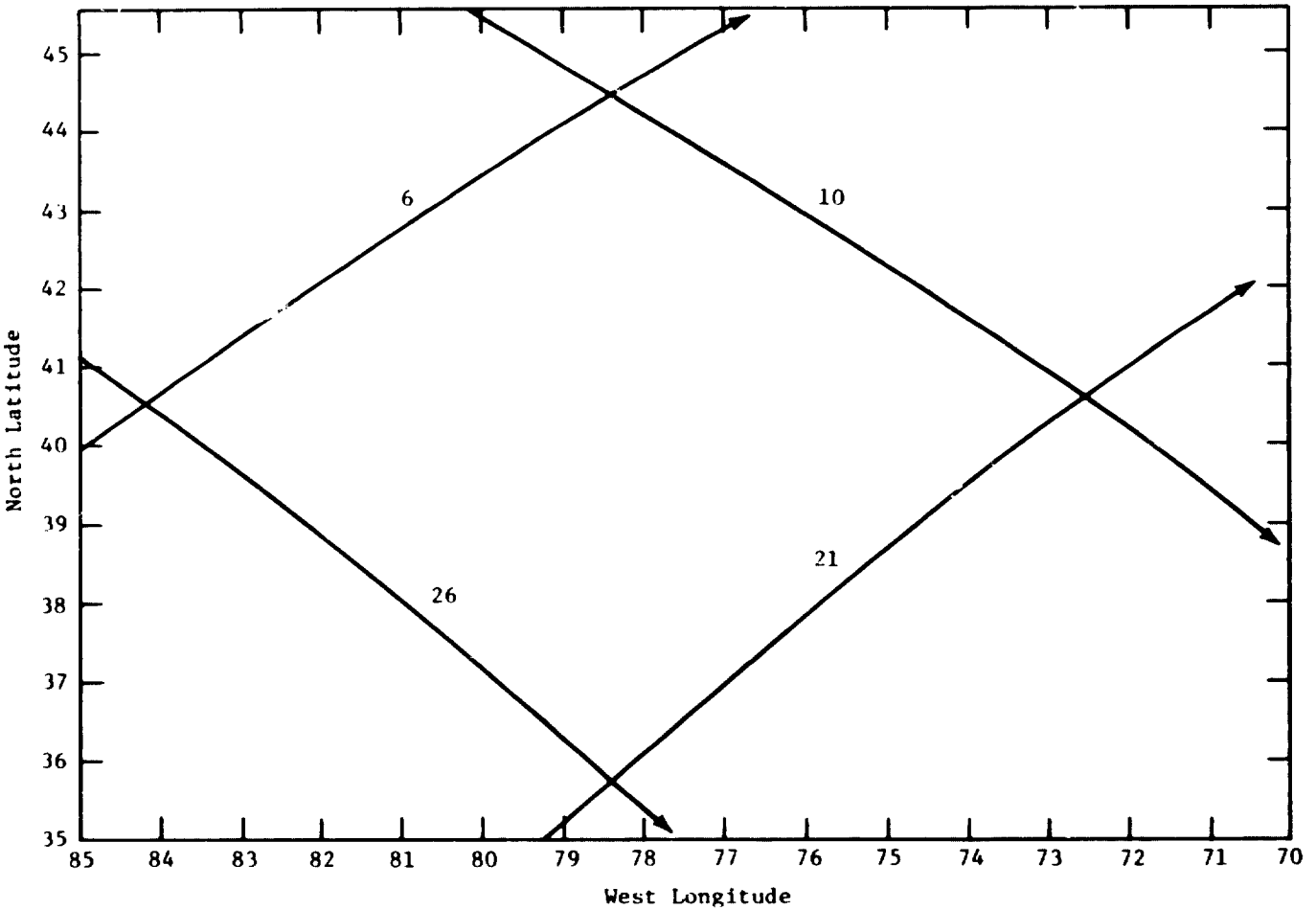

FIGURE 3-2
GROUND TRACK FOR ORBIT WITH TWO-DAY REPEAT CYCLE
(altitude = 349 km, inclination = 56°)

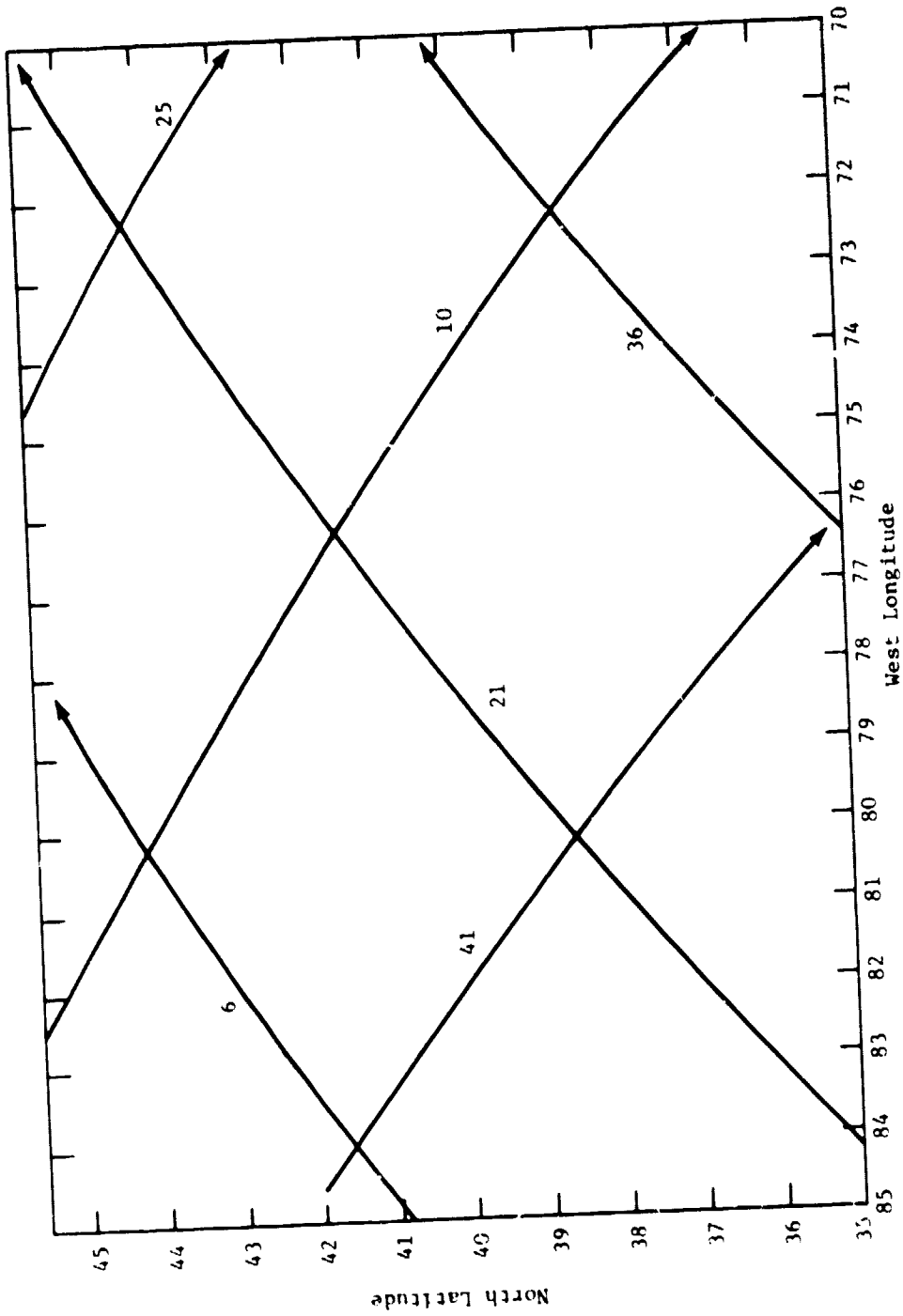

FIGURE 3-3
GROUND TRACK FOR ORBIT WITH THREE-DAY REPEAT CYCLE
(altitude = 399 k.m., inclination = 56°)

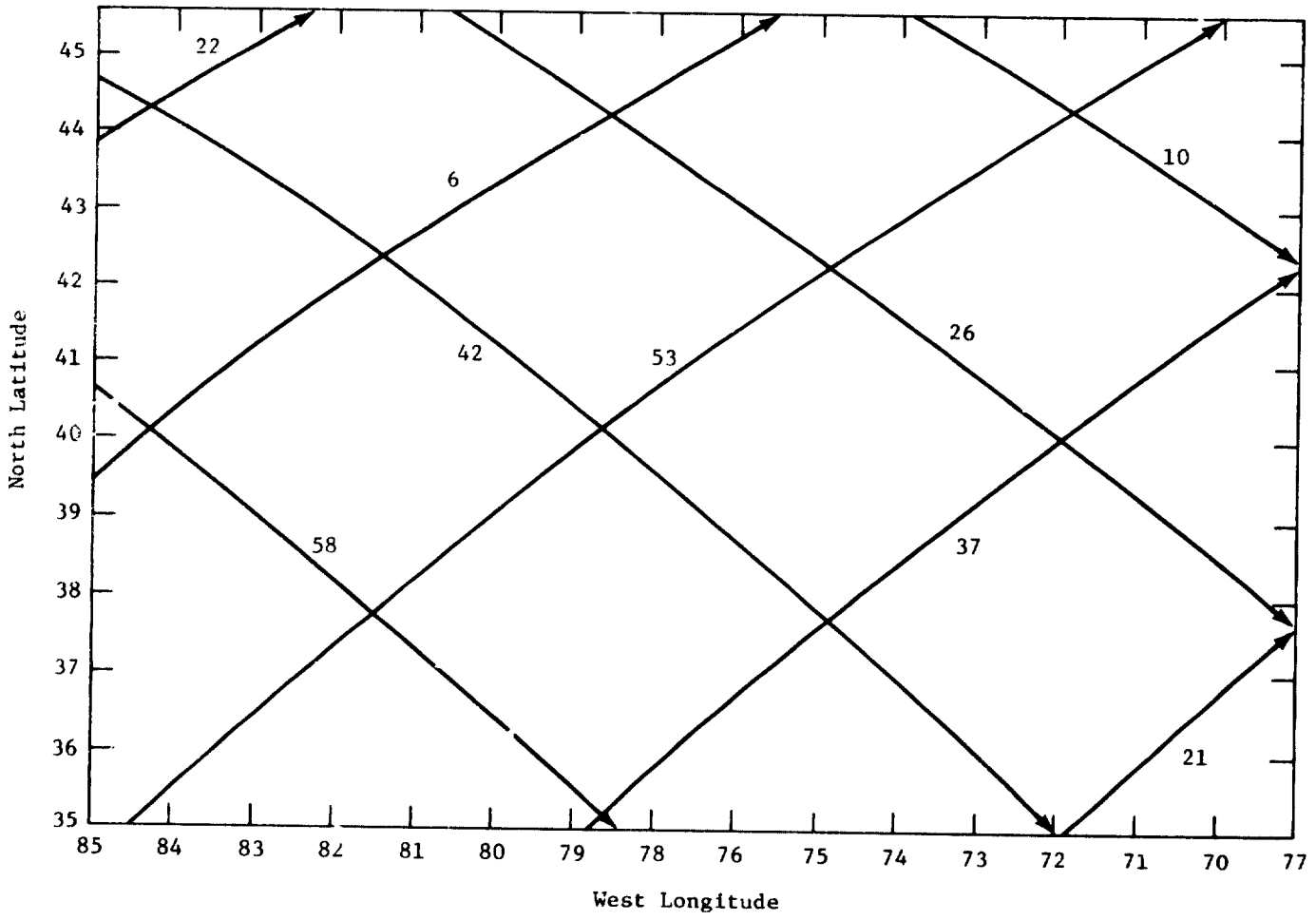

FIGURE 3-4
GROUND TRACK FOR ORBIT WITH FOUR-DAY REPEAT CYCLE
(altitude = 277 km, inclination = 57°)

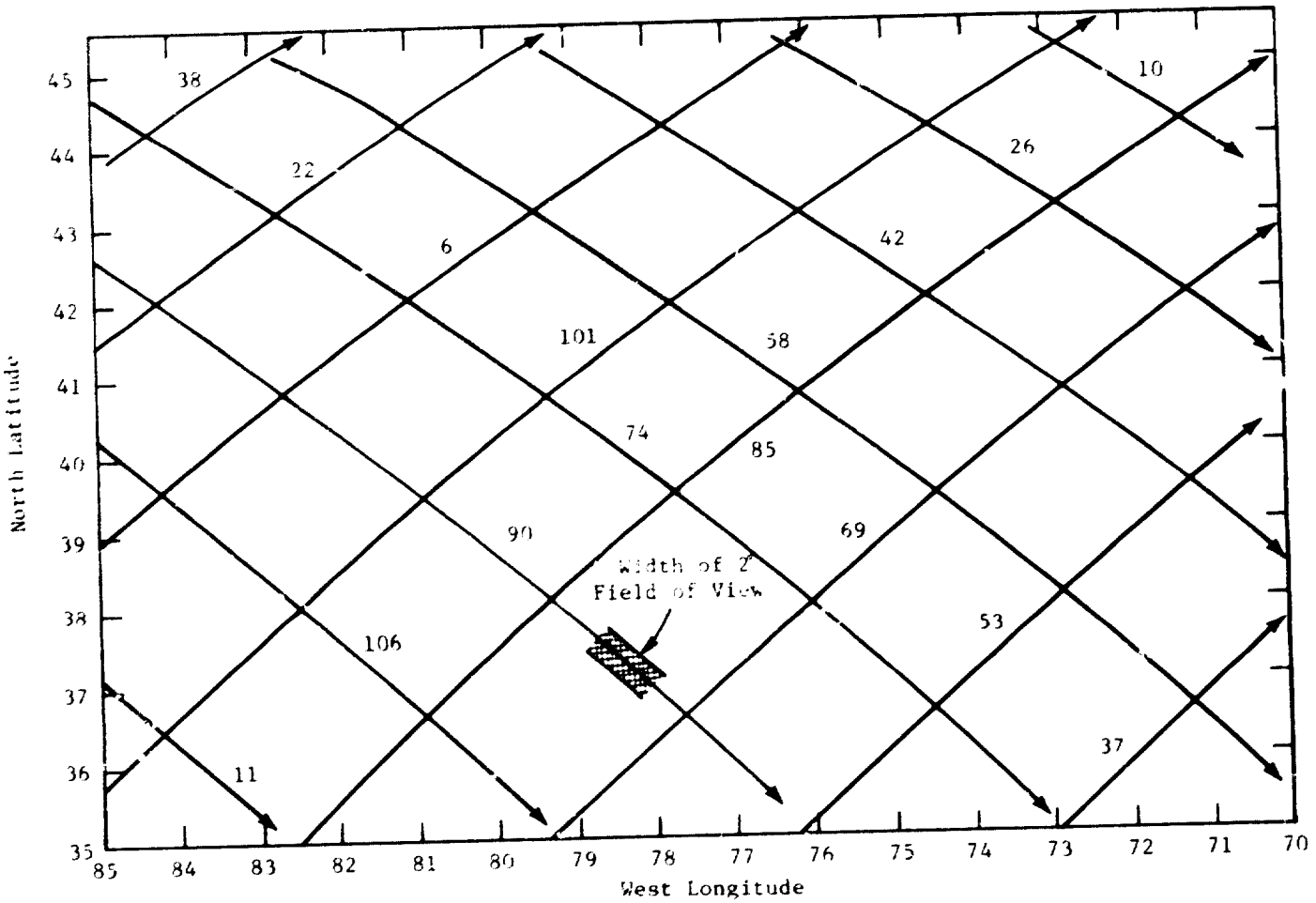

FIGURE 2
GROUND TRACK OF TYPICAL SHUTTLE ORBIT (ALTITUDE = 245 km, INCLINATION = 57°). EACH TRACK IS ASSOCIATED WITH THE NUMBER OF ORBITS SINCE THE START OF THE MISSION.

TABLE 3-I

ORBIT DATA

Altitude(km)	Inclination (°)	Repetition Factor	Repeat Cycle(days)	Nodal Movement Per Orbit	Orbits Per Repeat Cycle
492	45	15.00	1	24	15
349	56	15.50	2	23.23	31
399	56	15.33	3	23.48	46
277	57	15.75	4	22.86	63
245	57	15.86	7	22.70	111

One of the orbits (Figure 3-1) has an altitude higher than one might expect for Shuttle but is included both because it shows the control of orbit inclination on latitudinal coverage (no observations above 45° occur in the example) and because it has a one-day repeat cycle. In effect, this example orbit illustrates one extreme in the trade-off between spatial sampling density and frequency of sampling. The other extreme, for the proposed seven-day mission duration, is shown in Figure 3-5. The orbit has a seven day repeat cycle, about four times as much spatial sampling density as the one day repeat cycle case but only one seventh the frequency of sampling (since it takes seven days to complete the sampling pattern).

There are two factors which, along with the orbit parameters, determine the solar elevation history along the ground track of the orbit: the local time of the various observations and the declination of the sun as it varies with the seasons. The solar elevation is primarily of importance in determining the occasions on which the solar wavelength channel of the CIMATS sensor will have adequate radiation levels.

Variation from measurement to measurement of the local sun time is of significance since it indicates the amount of diurnal sampling which can be achieved during the mission. If the mission is sufficiently long that each hour of the day and night is sampled many times, the diurnal sampling is better than in the case of a sunsynchronous or nearly sunsynchronous orbit for which all observations at a particular point are made at the same local time.

Seasonal variations in the declination of the sun, and the movement of the orbit plane with respect to the Earth-Sun line determine the range of latitudes for which observations can be made at various times of the year. Figure 2-4 illustrates these limits for a 56° inclination orbit if 30° solar elevation is to be achieved. The Figure shows that missions as long as approximately 20 days can enjoy the maximum possible latitude coverage in one hemisphere or the other, as long as the launch date is chosen with care. The time of day of the launch is also important (in this case it was assumed that the first orbit crossed the equator at 12:00 noon). The Figure also shows that winter conditions limit the latitudes which can be covered. From November to March only latitudes up to 30° can be covered in the Northern hemisphere.

The field-of-view of the instrument adds slightly to the area covered over and above the sampling pattern of the orbit. For example, from an altitude of 400 km, the width of the CIMATS field of view (7°), measured in degrees of great circle arc is about 0.4°. The spacing of the orbit tracks in the most dense case, a seven-day repeat cycle, is about three degrees so the contribution of the field-of-view is small in comparison. Figure 3-5 illustrates the width of the field-of-view.

The orbit analysis model used to develop the figures for this section is described in Appendix A.

4.0 MODEL FOR STATISTICAL INTERPRETATION

This section discusses the capability of remote sensors, like MAPS and CIMATS, to measure pollution levels when flown on the Space Shuttle. This has been done by developing a method of quantifying the sensor's performance as a function of the individual instrument's design parameters. In particular, the impulse response functions of the instruments are derived. These response functions are used along with consideration of the fact that the pollution distribution is a function of time as well as space. The important design parameters considered are:

1) Velocity of the ground track of the Space Shuttle,

2) Resolution (area on the ground viewed by the instrument),

3) Temporal response characteristics and response delay,

4) Time duration of individual observations and,

5) Spatial and temporal sampling of the region of interest.

These parameters are used, along with the instrument model, to develop methods for the determination of the uncertainty associated with the observations.

Characterization of the uncertainty in the observations requires information on three factors: 1) the uncertainty in individual observations as determined by the performance of the instrument and data reduction methods; 2) the uncertainty associated with incomplete sampling of the scene in space and time; and 3) uncertainty associated

with instrument response to spatial and temporal variability in the scene. Identification of instrument uncertainty (both bias and random) is relatively straightforward as a result of laboratory calibration and field testing. Sampling uncertainties are somewhat more complex, however, since they involve both the sampling characteristics provided by orbit, as well as the natural spatial and temporal variability of the pollutants. Models of the spatial and temporal response of the instrument response function were carried out to complete the analysis. Calculation of the overall uncertainty in the pollution estimates involves a sum of squares calculation assuming a linear additive model using the contributions from 1), 2) and 3) above. Discussion of the overall uncertainties concludes the results of this section.

4.1 Spatial Impulse Response Function

A number of parameters characterize the capability of a remote sensor to respond to the variations in the pollution it is attempting to detect. These include:

velocity of the ground track	- V(km/seconds)
time constant of the instrument*	- τ_I(seconds)
full angle field-of-view	- Ω(radians)
altitude of the spacecraft	- A(kilometers)
footprint of the field-of-view	- D = ΩA

Each element which enters the field-of-view acts like a unit step function whose amplitude indicates the absolute amount of

---

*Assumes the instrument response to a step function grows as $1-e^{-t/\tau}$.

pollution in that element region. During its time in the field-of-view, (D/V), that element produces a response of the form

$$1-e^{-t/\tau_1}$$

After the element has moved outside the field-of-view, the response approaches zero according to

$$e^{-t/\tau_1}$$

As the footprint progresses along the orbit path, each successive small area interacts with the changed concentration and alters the output of the sensor.

If the pollution level is described as g(x), then the contribution from elements in the field-of-view at any place x is given by [1,2]

$$f_1(x) = \frac{1}{D} \int_{x-D}^{x} g(x') \left[1 - \exp\left(-\frac{x-x'}{V\tau_1}\right)\right] dx' \qquad (1)$$

Similarly, the contribution of the elements which have moved out of the field-of-view is given by

$$f_2(x) = \frac{1}{D} \left[\exp\left(\frac{D}{V\tau_1}\right)-1\right] \int_{0}^{x-D} g(x')\exp\left(\frac{x'-x}{V\tau_1}\right) dx'. \qquad (2)$$

The total response of the sensor thus becomes

$$f(x) = \frac{1}{D} \int_{x-D}^{x} g(x') \left[1-\exp\left(-\frac{x-x'}{V\tau_1}\right)\right] dx'$$

$$+ \frac{1}{D}\left[\exp\left(\frac{D}{V\tau_1}\right)-1\right] \int_{0}^{x-D} g(x') \exp\frac{x'-x}{V\tau_1} dx'. \qquad (3)$$

Equation 3 is a convolution of two functions and can be rewritten as

$$f(x) = \int g(x') \; h_1(x-x') \; dx'$$

where

$h_1(x)$ is the spatial impulse response function and is given by

$$h_1(x) = \frac{1}{D}\left[1-\exp\left(-\frac{x}{V\tau_1}\right)\right]U(x)$$

$$-\frac{1}{D}\left[1-\exp\left(-\frac{x-D}{V\tau_1}\right)\right]U(x-D). \qquad (4)$$

U(x-D) here is a unit step function defined as

$$U(x-D) = \begin{cases} 0 & x<D \\ 1 & x>D \end{cases} \qquad (5)$$

Equation 4 is simplified further when expressed in terms of spatial frequencies. The frequency spectrum $H_1(j\omega_1)$ is the Fourier Transform of $h_1(x)$:

$$H_1(j\omega_1) = \int_{-\infty}^{\infty} h(x) \; e^{-j\omega_1 x} \; dx$$

$$= \frac{1 - e^{-j\omega_1 D}}{j\omega_1 D(1+j\omega_1 V\tau_1)} \; . \qquad (6)$$

Equation 6 can be plotted as a function of ω_1 after appropriate values of V, D and τ have been selected. To obtain a satisfactory level of signal against background noise, the time constants of 1 second and 10 seconds are being currently considered for CIMATS and MAPS, repsectively. The fields-of-view of the respective instruments

are 7° and 4.3° [3]. The Shuttle platform velocity, V, is approximately 7 km/sec. [2].

Equation 6 was evaluated with all the appropriate values of the parameters listed above. A plot of $H_1(j\omega_1)$ with varying spatial frequencies is given in Figure 4-1. If the half power bandwidth of a system is defined as the frequency where the system response function falls to 0.707 of its maximum value, then it is evident from the figure that the spatial resolutions of CIMATS and MAPS are 150 km and 100 km, respectively. It is interesting to compare these figures with the instantaneous field-of-view of the two instruments, unaffected by the satellite velocity and instrument time constant (CIMATS ~50 km and MAPS ~30 km from an altitude of 400 km). A considerable increase in the effective field-of-view along the orbit track is evident for each instrument (corresponding to poorer resolution along the orbit track). Cross-track resolution is unaffected by the dynamic response capabilities of the sensors.

4.2 Temporal Impulse Response Function

To determine the temporal impulse response function, the instruments can be represented by the block diagram as shown in Figure 4-2.

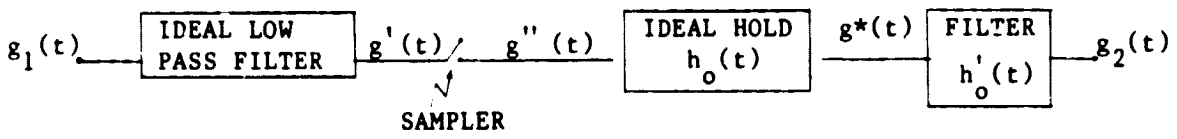

FIGURE 4-2

BLOCK DIAGRAM REPRESENTATIVE OF A TYPICAL SENSOR

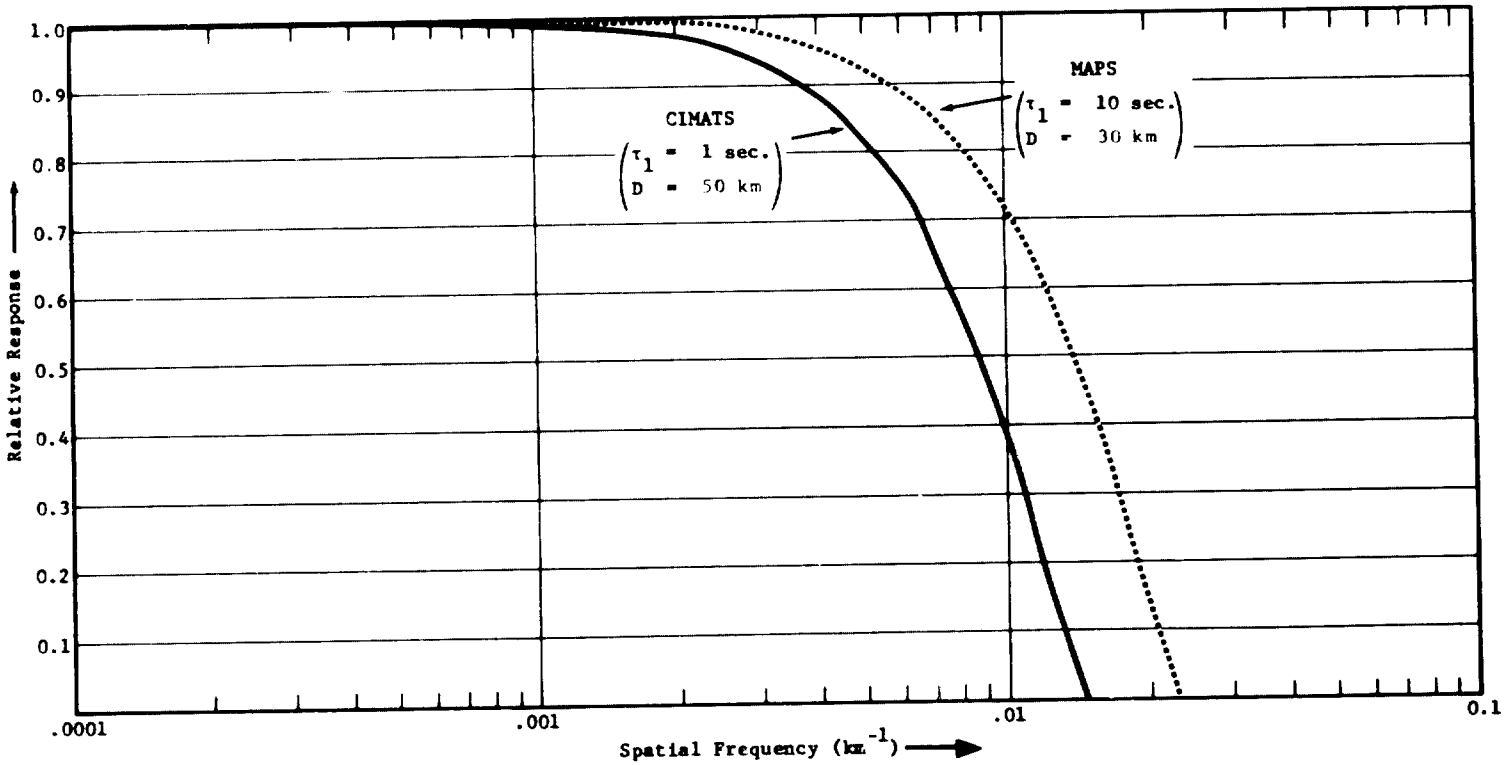

FIGURE 4-1
INSTRUMENT SPATIAL IMPULSE RESPONSE FUNCTION

The ideal low pass filter in the front end of the sensor limits the maximum frequency content in the pollution distribution to be observed by the sensor and aids in determining the optimum sampling rate. The bandwidth Δf of this filter is approximately given by [2]

$$\Delta f \approx \frac{1}{4\tau_1}$$

where

τ_1 is the electronic time constant of the instrument.

The output signal g'(t), which is limited to the frequency band 0 to Δf, is sampled at a constant frequency of $f_0 = \frac{1}{T_0}$, where $f_0 \geq 2\Delta f$. This sampling rate is required since to transmit a band limited signal of duration T_1 and maximum frequency f_m, it suffices to send a finite set of $2f_mT_1$ independent amplitude samples obtained by sampling the instantaneous amplitude of the signal at a regular rate of $2f_m$ samples/second. This is a statement of the so-called Nyquist criterion.

g"(t) in Figure 4-2 is a train of impulses given by

$$g''(t) = \sum_{n=o}^{T_1/T_o} g(nT_o)\,\delta(t-nT_o) \qquad (7)$$

where δ is the Dirac delta function.

T_o is the sampling interval and as discussed above is related to Δf and the electronic time constant by

$$T_o = \frac{1}{2\Delta f} = 2\tau_1. \qquad (8)$$

$g^*(t)$ is a sampled function consisting of short pulses, F_1, F_2,.... F_n, of equal duration τ_3 at equal intervals T_0. Thus, impulse response function of the hold circuit is given by

$$h_0(t) = U(t) - U(t-\tau_2) \text{ for all } \tau_2 < T . \qquad (9)$$

The last filter of the system gives a real time response and reflects the time constant (τ_1) of the system. Its impulse response function is given by

$$h'_0(t) = e^{-t/\tau_1} . \qquad (10)$$

Finally, the convolution of $h_0(t)$ with $h'_0(t)$ determines the temporal impulse response function. The temporal impulse response function $h_2(t)$ is given by

$$h_2(t) = h_0(t) * h'_0(t)$$

$$= \tau_1 \left[1-\exp\left(-\frac{t}{\tau_1}\right)\right]U(t)$$

$$+ \tau_1 \left[1-\exp -\left(\frac{t-t_2}{\tau_1}\right)\right]U(t-\tau_2) \text{ for all } \tau_2 < T . \quad (11)$$

The temporal frequency response function is the Fourier Transform of $h_2(t)$ and is presented by $H_2(j\omega_2)$:

$$H_2(j\omega_2) = \int_{-\infty}^{\infty} h_2(t)\, e^{-j\omega_2 t}\, dt$$

$$= \tau_1 \cdot \frac{1-e^{-j\omega_2\tau_2}}{j\omega_2(1+j\omega_2\tau_1)} \quad \text{for all } \tau_2 < T \qquad (12)$$

The function $H(j\omega_2)$ was evaluated for $\tau_2 = T_0$ and $0.5\ T_0$ and is illustrated in Figure 4-3. The poorer response is evident in

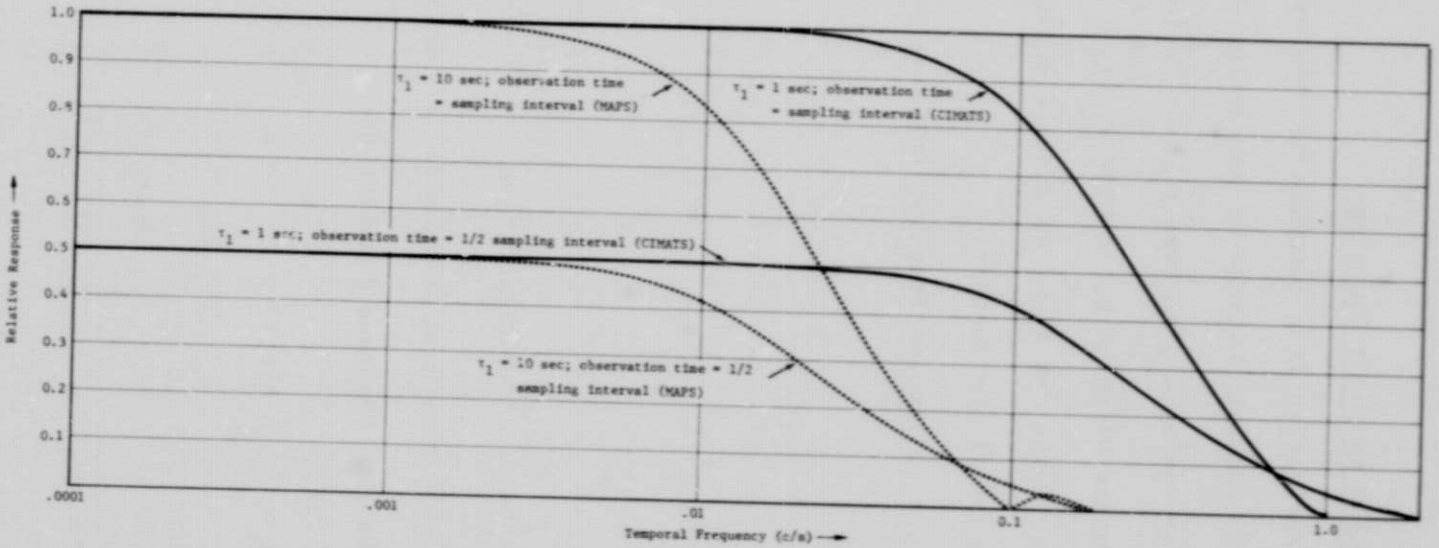

FIGURE 4-3
INSTRUMENT TEMPORAL RESPONSE FUNCTION

those cases where the observation time is smaller than the sampling interval.

4.3 Total System Impulse Response Function

The pollution distribution is a function of time as well as spatial variations. In general, because of meteorology, the pollution distribution at any point x_2, at time t_2, may be influenced by the pollution distribution of point x_1 at time t_1 ($t_1 < t_2$). The instrument responses in space and time, as derived above, can be considered as independent of one another.

Thus, the total system impulse response function represented as $h(x,t)$ is given by

$$h(x,t) = h_1(x) \cdot h_2(t)$$

$$= \left[\frac{1}{D}\left(1-e^{-x/V\tau_1}\right) U(x) - \frac{1}{D}\left(1-e^{-(x-D)/V\tau_1}\right) U(x-D)\right]$$

$$\cdot \left[\tau_1\left(1-e^{-t/\tau_1}\right) U(t) - \tau_1\left(1-e^{-(t-\tau_2)/\tau_1}\right) U(t-\tau_2)\right] \quad (13)$$

Taking the double Fourier Transform of Equation 13, we obtain the system bi-frequency impulse response function as

$$H(j\omega_1, j\omega_2) = \int_{-\infty}^{\infty}\int_{-\infty}^{\infty} h(x,t)\, e^{-j\omega_1 x} \cdot e^{-j\omega_2 t}\, dx\, dt$$

$$= \frac{1-e^{-j\omega_1 D}}{j\omega_1 D(1+j\omega_1 V\tau_1)} \cdot \tau_1 \cdot \frac{1-e^{-j\omega_2\tau_2}}{j\omega_2(1+j\omega_2\tau_1)} . \quad (14)$$

This formulation is applied to instrument performance evaluation in the next section.

4.4 Instrument Performance Evaluation

Let $g_1(x,t)$ be the input pollution distribution at any x, and t, and $g_2(x,t)$ be the instrument response to this input. To determine how accurately the original distribution is reproduced, a criterion relating the average power in the input and output pollution distributions may be used. The average power of a random process x(t) is given by

$$E\left\{x^2(t)\right\}$$

where

E is the expectation operator. The difference between the average power of $g_1(x,t)$ and $g_2(x,t)$ will be given by

$$= E\left\{g_1^2(x,t)\right\} - E\left\{g_2^2(x,t)\right\} \quad . \tag{15}$$

The power spectrum or a spectral density $S_{g_1}(\omega_1,\omega_2)$ of the process $g_1(x,t)$ is the Fourier Transform of its autocorrelation:

$$S_{g_1}(\omega_1,\omega_2) = \int_{-\infty}^{\infty}\int_{-\infty}^{\infty} R_{g_1}(\xi_1,\xi_2)\, e^{-j\omega_1\xi_1} \cdot e^{-j\omega_2\xi_2}\, d\xi_1\, d\xi_2 \tag{16}$$

where

$$R_{g_1}(\xi_1,\xi_2) = E\left\{g_1(x,t)g_1(x+\xi_1,\ t+\xi_2)\right\}. \tag{17}$$

From Equation 16, using Fourier inversion formula, it follows that

$$R_{g_1}(\xi_1,\xi_2) = \frac{1}{4\pi^2}\int_{-\infty}^{\infty}\int_{-\infty}^{\infty} S_{g_1}(\omega_1,\omega_2)\, e^{j\omega_1\xi_1}\, e^{j\omega_2\xi_2}\, d\omega_1\, d\omega_2. \tag{18}$$

With $\xi_1 = o$, and $\xi_2 = o$, the above yields an expression for the average power of the input distribution

$$E\left\{g_1^2(x,t)\right\} = \frac{1}{4\pi^2}\int_{-\infty}^{\infty}\int_{-\infty}^{\infty} S_{g_1}(\omega_1,\omega_2)\, d\omega_1\, d\omega_2. \tag{19}$$

Then, the difference ε becomes

$$\varepsilon = \frac{1}{4\pi^2}\int_{-\infty}^{\infty}\int_{-\infty}^{\infty} S_{g_1}(\omega_1,\omega_2)d\omega_1 d\omega_2 - \frac{1}{4\pi^2}\int_{-\infty}^{\infty}\int_{-\infty}^{\infty} S_{g_2}(\omega_1,\omega_2)d\omega_1 d\omega_2 \tag{20}$$

The spectral density $S_{g_2}(\omega_1,\omega_2)$ of the output $g_2(x,t)$ is dependent upon the system impulse response function and the spectral density of the input [4]. It is given by

$$S_{g_2}(\omega_1,\omega_2) = \left|H(j\omega_1,j\omega_2)\right|^2 S_{g_1}(\omega_1,\omega_2) . \tag{21}$$

So that

$$\varepsilon = \frac{1}{4\pi^2}\int_{-\infty}^{\infty}\int_{-\infty}^{\infty} S_{g_1}(\omega_1,\omega_2)\, d\omega_1\, d\omega_2$$

$$- \frac{1}{4\pi^2}\int_{-\infty}^{\infty}\int_{-\infty}^{\infty} H(j\omega_1,j\omega_2)^2 \; S_{g_1}(\omega_1,\omega_2)\, d\omega_1\, d\omega_2 \tag{22}$$

and the percent difference is given by

$$\% \;\varepsilon = 100 \cdot \left(1 - \frac{\int_{-\infty}^{\infty}\int_{-\infty}^{\infty} \left|H(j\omega_1,j\omega_2)\right|^2 S_{g_1}(\omega_1,\omega_2)\, d\omega_1\, d\omega_2}{\int_{-\infty}^{\infty}\int_{-\infty}^{\infty} S_{g_1}(\omega_1,\omega_2)\, d\omega_1\, d\omega_2}\right) \tag{23}$$

The difference of Equation 23 can be used as a part of the uncertainty analysis.

4.5 Use of A Theoretical Input Pollution Distribution Model

For a demonstration of the instrument error, $g_1(x,t)$ can be considered a product of two mutually exclusive functions $g(x)$ and $g_1(t)$ where $g(x)$ determines the spatial pollution distribution and $g_1(t)$ give the temporal pollution distribution.

Furthermore, the spatial distribution of pollutant concentrations $g(x)$ can be assumed to be a Gaussian distribution. This is a convenient assumption, and is used as a basis for air pollution models [5]. It is of the form

$$g(x) = \frac{1}{\sqrt{2\pi}\,\alpha} \exp\left[-\frac{\left(x-x_o\right)^2}{2\alpha^2} \right] \tag{24}$$

where x_o is the center of the pollution distribution (near the urban center), and α is a measure of the plume spread. The range of value of α (5 to 30 km) is typical of pollution sources ranging in the size from an interchange of several major highways to large cities like New York.

The temporal pollution distribution $g_1(t)$ can be modeled on the basis of a normal Markoff process with zero mean [6].

The autocorrelation function of a Markoff process is given by

$$R(\xi_2) = e^{-C\left|\xi_2\right|} \tag{25}$$

where C is a constant, representing the duration of periods of constant conditions. That is, every C seconds the atmosphere is assumed to have reached some stable state which persists for C seconds.

The spectral density of $g_1(t)$ is given by the Fourier Transform of $R(\xi_2)$ and is:

$$S_f(\omega_2) = \frac{2C}{4C^2+\omega_2^2} \tag{26}$$

Combining Equation 26 with the spectral density of Equation 21, we obtain the spectral density of our model of the input:

$$S_{g_1}(\omega_1,\omega_2) = \left| \int_{-\infty}^{\infty} \frac{1}{\sqrt{2\pi}\alpha} e^{-x^2/2\alpha^2} e^{-j\omega_1 x} dx \right|^2 \frac{2C}{4C^2+\omega_2^2}$$

$$= e^{-\omega_1\alpha} \frac{2C}{4C^2+\omega_2^2} \tag{27}$$

Finally, substitution of Equations 27 in Equation 23 determines ;

$$\% \ \varepsilon = 100 \left[1 - \frac{\int_{-\infty}^{\infty}\int_{-\infty}^{\infty} \left| H(j\omega_1, j\omega_2) \right|^2 e^{-\omega_1\alpha} \frac{2C}{4C^2+\omega_2^2} d\omega_1 \, d\omega_2}{\int_{-\infty}^{\infty}\int_{-\infty}^{\infty} e^{-\omega_1\alpha} \frac{2C}{4C^2+\omega_2^2} d\omega_1 d\omega_2} \right] \tag{28}$$

Equation 28 was evaluated for the MAPS and CIMATS design parameters. The constant C was assumed to take a value of 1000 seconds. The results for varying spatial variances in pollution spatial distributions are shown in Figure 4-4. To determine the effect of system temporal response separately, Equation 28 was computed considering

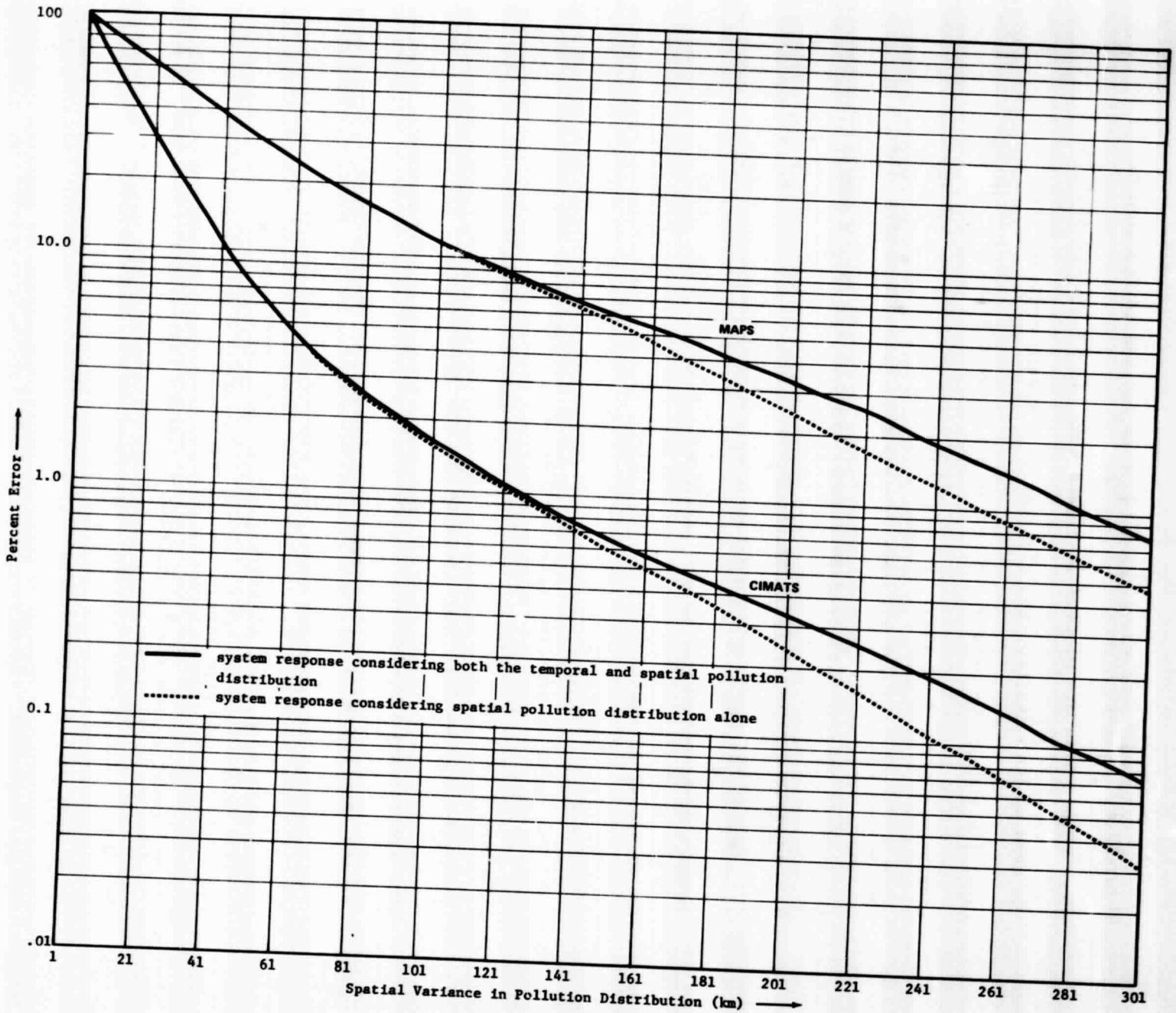

FIGURE 4-4
INSTRUMENT ERROR

$H(j\omega_1, j\omega_2) = H_1(j\omega_1)$ only; where $H_1(j\omega_1)$ is defined in Equation 6. These values also are plotted in Figure 4-4. It is evident that in the case of both instruments, the spatial response controls the total instrument response up to scales approximately the size of the instantaneous field-of-view. At much larger scales, up to 300 km, the spatial and temporal response contribution is about equal. The instruments operate with ignorably small error at the larger scales.

4.6 Uncertainty Due to Sampling Strategies

One of the key issues in determining the performance of remote sensors on-board Shuttle is the determination of the uncertainty in assessing pollution distributions because of the sampling distribution in space and time.

The sampling problem arises because the selection of the orbit and the inhibiting influence of clouds may make the spatial and temporal sampling less than adequate for the purpose of characterizing the spatial and temporal variability of the pollution. The adequacy of the sampling which is achieved is a function of the variability of the pollution in space and time. For a scene exhibiting little change with time, only infrequent observations are required.

For a scene with little spatial variability, a few observations at different points may be adequate to obtain statistically meaningful averages. The problem at hand, unfortunately, is characterized by a high spatial and temporal variability so that sampling limitations become important. It is the purpose of this subsection to quantify

the sampling by considering both that which can be achieved as well as the spatial and temporal variability in the pollution distribution.

The pollutants of interest may exhibit considerable spatial and temporal variability. In fact, different pollutants may exhibit different patterns of diurnal, seasonal and spatial variability. The pollution can therefore be regarded as a stochastic variable, with the pollution variations through each day being a record from the ensemble of all possible records. Let $\mu(t)$ represent the ensemble mean of $P_i(t)$, the pollution at time of the day, t on the i^{th} day. Then, the average pollution for N days at time t is

$$\mu(t) = \frac{1}{N} \sum_{i=1}^{N} P_i(t) \qquad (29)$$

Note that $\mu(t)$ is not independent of time because of the diurnal variations, and therefore, the process is a nonstationary stochastic process.

Integrating Equation 29 over the times of the day that instruments are capable of taking measurements, we obtain the time average pollution for N days. This is given by

$$\mu = \frac{1}{T} \int_{\text{time of the day}} \mu(t)dt \quad . \qquad (30)$$

Since Shuttle will be visiting one place only a finite number of times in N days, Equation 30 is rewritten as a sum:

$$\mu = \frac{1}{n} \sum_{j=1}^{n} \overline{P(t_j)} \qquad (31)$$

where

t_j is the j^{th} hour

$$n = \frac{24N}{\Delta t} \quad ,$$

$$\Delta t = t_{j+1} - t_j$$

Δt will be determined by the orbit parameters since they control the time between passes over the same place. Ideally, one would like to keep Δt as close as possible to the sampling interval given by Nyquist criterion, which may be impossible to achieve considering large variations in pollution diurnal cycles (see Section 4.2). For example, if the temporal variability of the scene is on the order of a day, which is not uncommon, the Nyquist criterion requires that samples be made on a scale of fractions of a day. It is unlikely that samples can be made with this temporal density. Therefore, the estimate of the average pollution at time t_j, $\hat{\mu}(t_j)$ may only be available from a single measurement taken at the j^{th} hour of the i^{th} day, $P_i(t_j)$. Let the variance of this single estimate be σ, defined as

$$\text{Var}\left[\hat{\mu}(t_j)\right] = \sigma^2(t_j) \tag{32}$$

then the estimate of the ensemble average over N days will be given by

$$\hat{\mu} = \frac{1}{n} \sum_{j=1}^{n} \mu(t_j) \tag{33}$$

and the variance of this pollution estimate, $\hat{\mu}$, will be [7]

$$\text{Var}\ [\hat{\mu}] = \frac{1}{n^2} \sum_{j=1}^{n} \sigma^2(t_j)$$

$$+ \frac{1}{n^2} \sum_{\substack{i=j \\ i=1,\ j=1}}^{n} \sigma(t_i)\, \sigma(t_j)\ \rho(i-j) \qquad (34)$$

where $(i-j)$ is the correlation between the pollution estimates $\hat{\mu}(t_j)$ and $\hat{\mu}(t_i)$ made at different times.

This analysis can be carried further using the following assumptions:

- the samples over the period are uniformly distributed over the time of the day,
- the variance in any pollution estimate is σ^2 and,
- the correlation between pollution estimates can be assumed to be of exponential form, i.e.,

$$(i-j) = e^{-k\alpha'} \qquad (35)$$

where

k is the index representing the k^{th} repeat cycle, and takes values between 0 and n. n is the number of repeat cycles in a time period of interest and equals the number of samples of a place in that time period.

α' is tne correlation coefficient/repeat cycle. If M represents the number of days/repeat cycle, and α is assumed to be the correlation coefficient for one day, then

$$\alpha' = M\alpha$$

Under these conditions, Equation 34 becomes [8]:

$$\text{Var}\,(\hat{\mu}) = \frac{\sigma^2}{n} + \frac{2\sigma^2}{n^2} \sum_{k=1}^{n-1} (n-k)\, e^{-k\alpha'}$$

$$= \frac{\sigma^2}{n} + \frac{2\sigma^2}{n^2} \frac{(n-1)e^{\alpha'} - n + e^{-(n-1)\alpha'}}{(e^{\alpha'}-1)^2} \qquad (36)$$

Equation 36 can be used to generate a set of curves for different values of n, M and α' which illustrate the variance in estimates (in units of σ) for various mission durations, repeat cycles and pollution correlations. Curves developed from this equation are shown in Figures 4-5 through 4-7. The mission durations considered in the examples are 7, 15 and 30 days. The data pertaining to 15 and 30 day missions are included for comparison to illustrate the value of missions longer than the expected 7-day Shuttle missions. The correlation of pollution on two successive days is indicated by ρ. The correlation coefficient, ρ, for one day is determined from using Equation 35, and is given by

$$\alpha = -\ln(\rho) \qquad (37)$$

Upon examination of Figures 4-5 through 4-7, it is clear that for a very high correlation of pollution of two successive days, the uncertainty in the estimate of pollution in units of σ is not significantly reduced by making a large number of samples. On the other hand, for a highly varying pollution scene, the correlation of pollution on two successive days is low, and the potential reduction

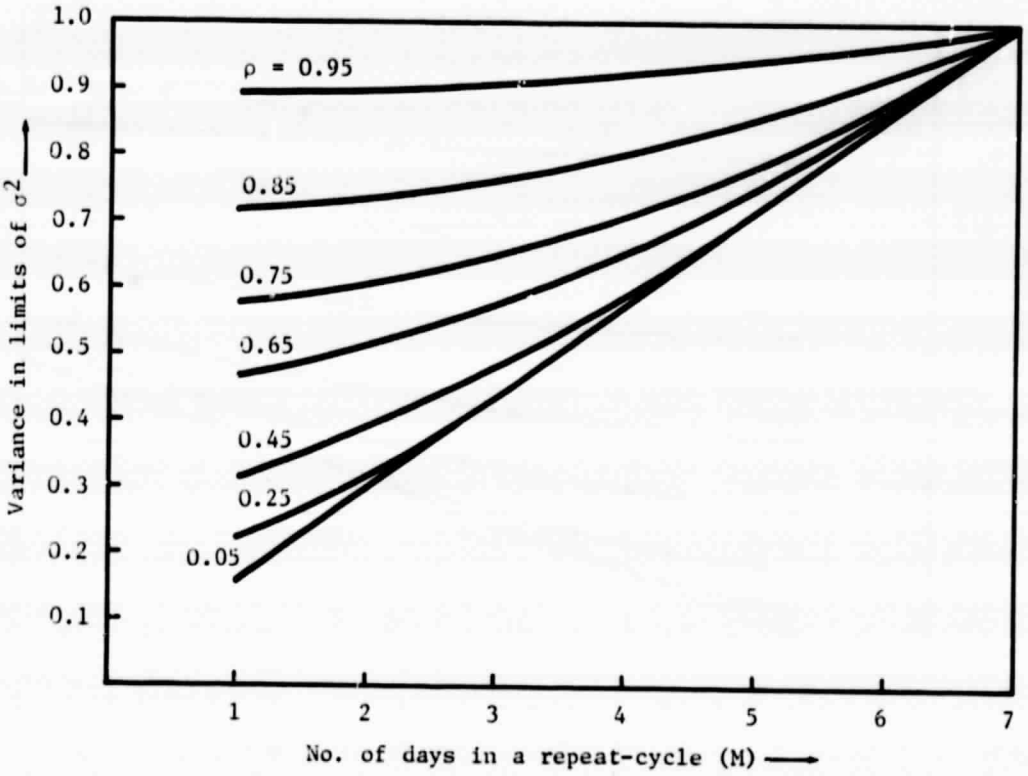

FIGURE 4-5
ERRORS DUE TO SAMPLING IN A 7 DAY MISSION

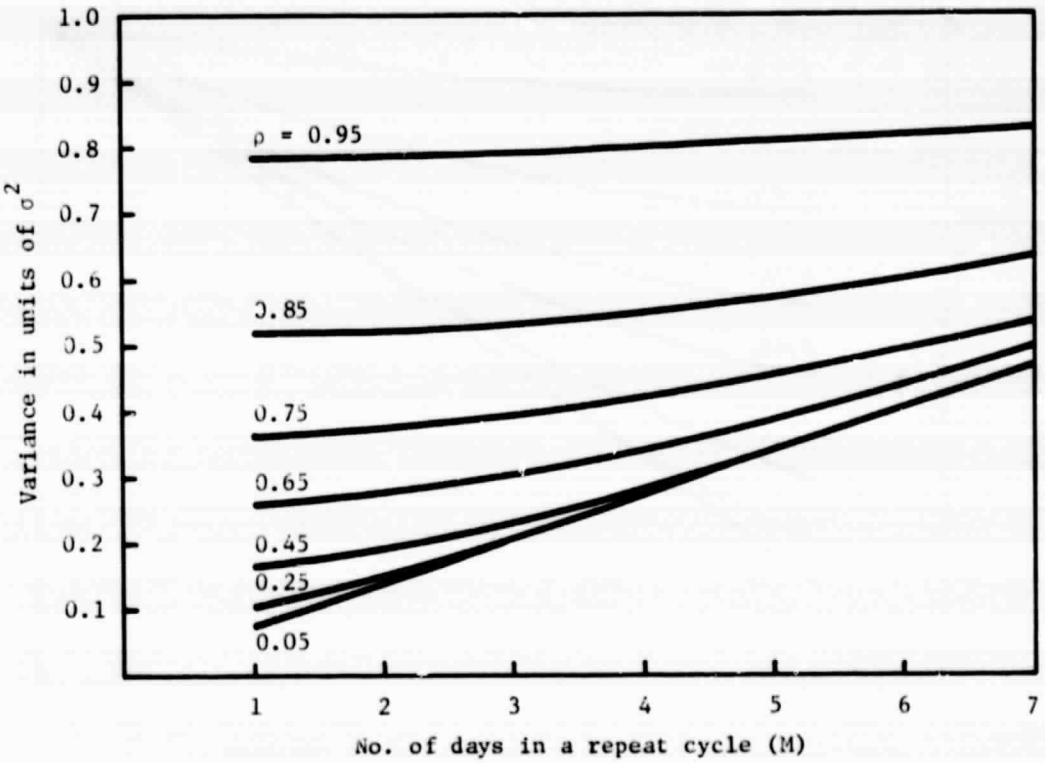

FIGURE 4-6
ERRORS DUE TO SAMPLING IN A 15 DAY MISSION

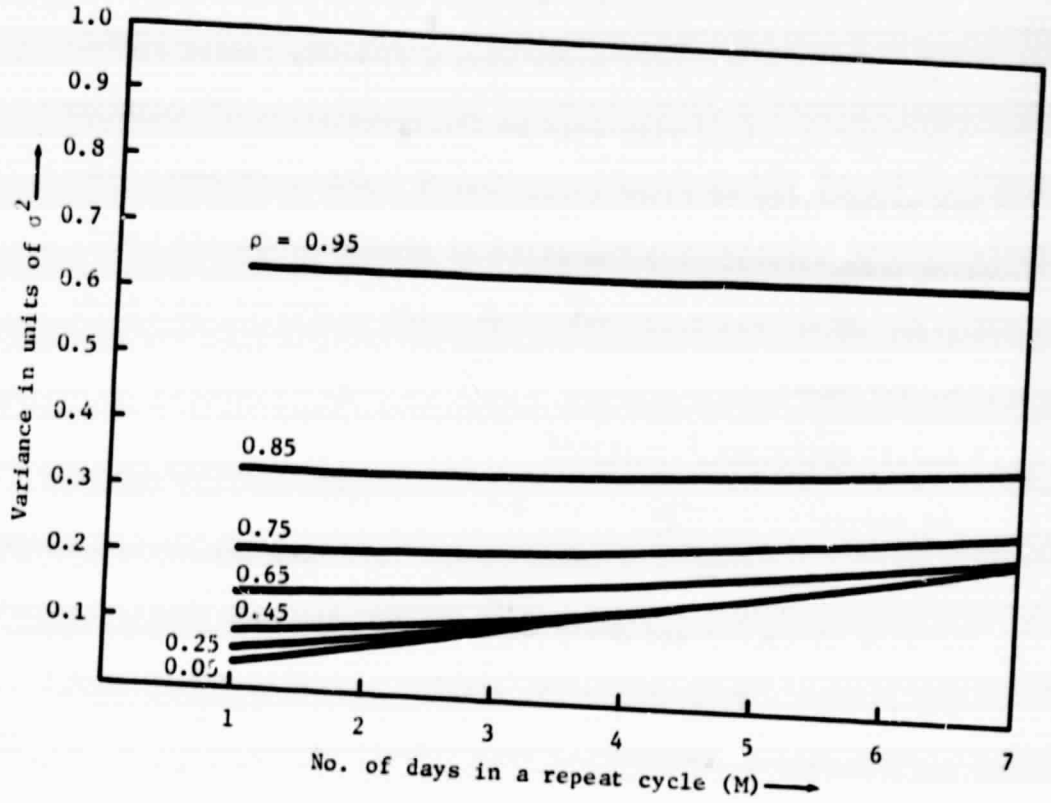

FIGURE 4-7
ERRORS DUE TO SAMPLING IN A 30 DAY MISSION

in the uncertainty in the estimate of pollution provided by a single observation is more pronounced.

4.7 Application of The Analytical Methods

The statistical tools developed in the previous sections can now be used collectively to determine the data quality which might result from a real mission. For example, it was found in Section 3 that a typical Shuttle orbit might have a five-day repeat cycle. This information, along with data on the correlation of pollution and the probability of cloud cover, can be used to estimate the sampling uncertainty. The inability of CIMATS to operate under conditions other than relatively high solar elevation angles can also be included.

4.7.1 Pollution Statistics

An extensive listing of air quality statistics were obtained from the Environmental Protection Agency [9]. The data were provided in the form of hourly and daily averages of pollution levels for July and August 1974. From this data, weekly, bi-weekly and monthly means ($\hat{\mu}$) and standard deviations (σ) were computed using conventional statistical methods. In addition, the correlations were also computed. The data appear in Table 4-I. The correlation computation was carried out using the method normally used in regression analysis. That is, [10]

$$\rho = \frac{n\sum x_{i+i}x_i - \sum x_{i+i}\sum x_i}{\left\{\left[n\sum x_{i+i}^2 - \left(\sum x_{i+i}\right)^2\right]\left[n\sum x_i^2 - \left(\sum x_i\right)^2\right]\right\}^{1/2}} \qquad (38)$$

TABLE 4-I

CARBON MONOXIDE POLLUTION DATA FOR A TYPICAL URBAN LOCATION [9]
(FOR THE MONTH OF AUGUST 30, 1974 AT GREENPOINT AVENUE,
NEW YORK, NEW YORK)

AVERAGING PERIOD	MEAN* (ppm)	STANDARD DEVIATION (ppm)	CORRELATION
7 days	3.36	1.20	0.46
15 days	3.34	1.19	0.45
30 days	3.35	1.20	0.45

where all sums range from 1 to n, the number of entries (for example, for a 30 day mission, the number of entries will be 30). Thus, the coefficient ρ represents the correlation between each measurement and the next successive one.

4.7.2 Use of the Data

The standard deviation and correlation data of Table 4-I have been used to compute the sampling uncertainty as a function of days per repeat cycle. The uncertainty due to sampling is

$$\frac{\text{Var}\,(\hat{\mu})}{\hat{\mu}} \times 100 \qquad (39)$$

Use of Equation 39 and Table 4-I result in Table 4-II, which is an example of the magnitude of sampling uncertainty which might occur in attempting to make estimates of the pollution in the New York city area, assuming that an IR sensor, unaffected by solar limitations is used. A 50% chance of cloudiness was assumed, based on the results of Appendix B. The sampling uncertainty for a mission of the expected duration (7 days) ranges from 20 to 36 percent, depending on the number of days in the repeat cycle of the orbits. However, for a mission of a month, the sampling uncertainty is reduced to the range of 10 to 22 percent, depending on the number of days per repeat cycle. As described in Section 3, the one-day repeat cycle provides the smallest sampling error. However, the orbit which produces a one-day repeat cycle is also the one which results in the poorest coverage of the area of interest.

TABLE 4-II

PERCENT SAMPLING UNCERTAINTY IN NEW YORK AS A FUNCTION OF DAYS PER REPEAT CYCLE (INCLUDING 50% CHANCE OF CLOUDINESS)

REPEAT CYCLE (days)	PERCENT ERROR* MISSION DURATION (days)		
	7	15	30
1	20.14	14.25	10.22
2	25.16	17.41	12.38
3	30.32	20.79	14.73
4	35.77	23.91	16.92
5	35.77	26.72	18.89
6	35.77	29.26	20.69
7	35.77	31.61	22.35

*EQUAL TO $\frac{\sqrt{\text{VAR}\,(\hat{\mu})}}{\hat{\mu}} \times 100$

4.7.3 Total System Performance

Three major elements make up the total uncertainty in estimates of pollution. They are: the radiometric uncertainty imposed by the instrument performance, uncertainties dictated by the spatial and temporal response functions of the instrument, and the sampling uncertainty. Under the assumption that these uncertainties are independent, and they appear to be, then the data quality is defined by a root sum of squares calculation. The total uncertainty is given by

$$\% \text{ uncertainty} = \left\{ \frac{\sigma_1^2}{L} + \frac{\sigma_2^2}{L} + \sigma_3^2 \right\}^{1/2} \qquad (40)$$

where L is the number of observations during the mission

σ_1: uncertainty in individual estimates

σ_2: uncertainty associated with response

σ_3: sampling uncertainty (derived from Table 4-II)

Table 4-III illustrates the total system uncertainty for various mission lengths and repeat cycles. As in the data of Table 4-II, 50 percent cloud cover is assumed. Other assumptions used in the analysis are that each pollution estimate has an uncertainty of 50 percent and that response uncertainties may be as high as 10 percent (based on Figure 4-4).

An expected result appears immediately; mission duration has a significant impact on the uncertainties, the shorter repeat cycle

TABLE I

TOTAL UNCERTAINTY (IN PERCENT) IN POLLUTION ESTIMATES
ASSUMING 50% CHANCE OF CLOUD COVER AND 50% UNCERTAINTY
IN INDIVIDUAL POLLUTION ESTIMATES

	MISSION DURATION (days)		
REPEAT CYCLE (days)	7	15	30
1	27.9	19.4	13.8
2	37.1	25.5	18.1
3	45.1	30.9	21.8
4	52.6	35.6	25.2
5	56.0	39.8	28.1
6	59.2	43.5	30.8
7	62.3	47.0	33.3

orbits exhibiting the best data quality. Conversely, these short repeat cycle orbits have the poorest density of sampling of the region of interest, as shown in figures 3-1 through 3-5. The mission designer has the choice, then, of attempting to achieve the best possible data but for limited locations. Alternatively, he may choose to gain the best possible spatial sampling of the region (as illustrated in Figure 3-5) at the expense of data quality at individual locations.

Clearly, a considerable number of assumptions have been included in the analysis above (frequency of cloudiness, uncertainty of individual pollution estimates, etc.) It was the object of this particular sub-section to illustrate the methods to be used in analyzing sensor/orbit performance. Additional analysis would be required if the assumptions were to be modified.

REFERENCES

1. L. J. Duncan, E. J. Friedman, E. L. Keitz and E. A. Ward, "An Airborne Remote Sensing System for Urban Air Quality," The MITRE Corporation, MTR-6601, February 1974.

2. A. Ghovanlou and E. Friedman, "Evaluation of the Airborne Air Pollution Remote Sensor," The MITRE Corporation, MTR-6795, March 1975.

3. Information on MAPS derived from a private communication with H. Reichle, Langley Research Center, May 27, 1977. Data on CIMATS appears in Section 2.

4. J. B. Thomas, Introduction to Statistical Communication Theory, John Wiley and Sons, Inc., pp. 144, 1969.

5. W. B. Johnson, F. L. Ludwig, W. F. Dabberdt and R. J. Allen "An Urban Simulation Model for Carbon Monoxide" Journal of the Air Pollution Control Association, Vol 23, No. 6, June 1973.

6. A. Paopoulis, Probability, Random Variables, and Stochastic Processes, McGraw-Hill, pp. 535, 1965.

7. E. J. Friedman, J. N. Gupta, R. G. Henderson, M. E. Lopez and H. J. Sheetz, "Evaluation of Earth Radiation Measurements by Satellites," The MITRE Corporation, METREK Division, MTR-7410, April 1977.

8. J. S. Bendat and A. G. Piersol, Measurement and Analysis of Random Data, John Wiley and Sons, pp. 344, 1958.

9. Obtained from National Aerometric Data Bank, U.S. Environmental Protection Agency, Office of Air Quality Planning and Standards, Research Triangle Park, North Carolina.

10. P. Hoel, Introduction to Mathematical Statistics, pp. 165, Wiley, New York, 1962.

5.0 USER INFORMATION NEEDS

The value of the Space Shuttle as a platform for remote sensing of atmospheric pollution will require that the data be of sufficient quality to satisfy the needs of potential users. There are basically three classes of users for data of this type. They include the general public, regulatory agencies and scientific groups. It is clear that both the standards for data quality and the format of presentation of the data will vary with the users. For example, the general public may be satisfied with relatively low quality data which depicts the general location and movement of pockets of high pollution levels. This data could be further supplemented by information of the potential for air stagnation, low level inversions or other meteorological phenomena which would tend to produce or prolong periods of poor air quality. There would also be, no doubt, an interest in determining the transport of pollutants or their precursors from city to city.

Scientific or regulatory users have much more specific requirements for data quality both in terms of accuracy and completeness of the sampling. In order to improve our understanding the transport, production and fate of pollutants, detailed studies will be required. The contribution to these studies which can be made by remote sensors on spacecraft is limited by their frequency of spatial and temporal sampling, frequent interference from clouds, relatively poor spatial resolution, limited capacity to resolve layers of the

troposphere and temporal gaps between missions. Sections, 2, 3, and 4 of this report define in detail the source and magnitude of the various limitations which would be encountered in attempting to apply the instruments of interest, MAPS and CIMATS, to scientific or regulatory functions. This section includes a discussion of the needs which currently exist for regional air quality data for scientific or regulatory purposes and a discussion of the data standards which would satisfy the public's demand for general air quality information. Section 6 compares these needs with expected performance and concludes with a set of recommendations for making the suggested missions more able to meet the requirements.

5.1 Users of Regional Data

An extensive study of the users and needs for local and regional air quality monitoring in the troposphere has recently been completed by the National Academy of Sciences [1]. This study provides the best and most comprehensive treatment of the topic. Table 5-I presents a summary of the results showing which of the various users have interests in four basic categories of needs. News media have an across-the-board need for information on important features of regional air pollution.

5.2 Measurement Requirements

The various groups interested in regional air pollution data do not have the same requirements in terms of species measured and geographical or temporal scales. The subsections below give

TABLE 5-I

USERS AND NEEDS FOR LOCAL AND REGIONAL
AIR QUALITY MONITORING IN TROPOSPHERE[1]

PRINCIPAL USERS	BASIC NEEDS			
	NEAR SURFACE SENSING (LOCAL)	REGIONAL AIR QUALITY DATA	PREDICTIVE MODEL INPUTS	MAJOR POINT SOURCE EMISSIONS
U. N. organizations	X	X	X	X
Federal agencies				
EPA	X	X	X	X
AEC			X	
NOAA			X	
DOT		X	X	
HEW	X	X		
NSF		X	X	
State and local agencies				
Regulatory	X	X	X	X
Planning	X	X		
Resource	X	X	X	X
Regional air pollution control boards	X	X	X	X
Environmental consultants	X	X	X	X
Engineers and architects	X	X	X	X
Research and scientific investigators	X	X	X	X
Medical and nursing professions	X	X		X
Public-interest groups	X	X		X
Industrials	X	X	X	X
News media	X	X	X	X

a summary of the compounds recommended for measurement or which have actually been measured in the various programs. The data have been extracted from a recent MITRE report [2].

5.2.1 Air Pollution Species to be Monitored

A summary of the air pollutants either recommended for measurement or actually measured in various regional studies is presented in Table 5-II. The difference in recommendations which exist among the references derive from their particular goals:

- National Academy of Sciences [1] - generalized tropospheric monitoring,
- Sulfate Regional Experiment [3] - investigation of sulfate formation from power plant emissions.
- Stanford Research Institute [4] - remote sensing of regional pollutants,
- Regional Air Monitoring System/Regional Air Pollution Study [5] - generalized urban and regional air quality,
- Los Angeles Reactive Pollutant Program [6] - validation of mathematical models of air pollution photochemistry in the Los Angeles area.
- Environmental Protecton Agency/Oxidant Study [7] - investigation of rural oxidant levels as related to urban hydrocarbons and,
- Battelle Columbus Laboratories [8] - formation and transport of ozone in nonurban areas.

5.2.2 Horizontal and Vertical Measurement Spacing

The horizontal or vertical measurement spacing selected for regional pollutant measurement must be on a scale which is commensureate with the scale of geographical changes in pollutant concentrations. Except for precise scientific investigations, the changes

TABLE 5-II

SPECIES RECOMMENDED OR ACTUALLY MEASURED IN VARIOUS REGIONAL STUDIES

SPECIES	NAS (1)		SURE (3)		SRI (4)		RAMS/RAPS (5)		LARPP (6)		EPA/OXIDANT (7)		BATTELLE (8)	
	RECOMMENDED	ACCURACY	RECOMMENDED	ACCURACY	RECOMMENDED	ACCURACY	MEASURED	ACCURACY	MEASURED	ACCURACY	MEASURED	ACCURACY	MEASURED	ACCURACY
Carbon Monoxide (CO)	X	10ppb			X	10ppb	X	NS	X	NS			X	NS
Formaldehyde (H_2CO)	X	1ppb			X	1ppb								
Halogens	X	1ppb												
Ammonia (NH_3)	X	10ppb	X	NS*	X	10ppb								
Sulfur Dioxide (SO_2)	X	10ppb	X	NS	X	10ppb	X	NS	X	NS				
Hydrogen Sulfide (H_2S)	X	0.1ppb	X	NS			X	NS						
Nitrogen Oxides (NO_x)	X	10ppb							X	NS	X	NS	X	NS
Peroxyacetyl nitrates (PAN)	X	10ppb												
Hydrocarbons	X	1ppb			X	est 1ppb	X	NS	X	NS	X	NS		
Ozone (O_3)	X	10ppb	X	NS	X	10ppb	X	NS	X	NS	X	NS	X	NS
Mercury (Hg)	X	10^{-2}ppb												
Nitric Oxide (NO)			X	NS			X	NS	X	NS	X	NS	X	NS
Nitrogen Dioxide (NO_2)			X	NS							X	NS	X	NS
Aerosols or Particulates			X	NS			X	NS	X	NS				
Methane (CH_4)					X	0.5ppm	X	NS			X	NS	X	NS
Hydrogen Chloride (HCl)					X	0.5-1ppm								
Non-Methane Hydrocarbon (NMHC)									X	NS	X	NS	X	NS
Total Sulfur (S)							X	NS						
Acetylene (C_2H_2)											X	NS	X	NS
Ethylene (C_2H_4)													X	NS
Ethane (C_2H_6)													X	NS
Fluorocarbon-11 (CCl_3F)													X	NS
Carbon Tetrachloride (CCl_4)													X	NS

*NS: Not stated

occurring in small cells or pockets of pollution with dimensions measured in meters or tens of meters are not generally of concern in regional studies.

Rather, regional studies are directed toward the broad scale effect produced over a wide area by an entire urban plume or large power plant plume. This fact has lead to the conclusion [4] that, "Regionally, horizontal resolution in the range of 10 km to 100 km would satisfy most needs."

Most regional experiments which have been proposed or conducted to date do not achieve the spacing suggested above. The principal reason for this is economic. The cost of aircraft or ground-based equipment, personnel and operations for such an extensive network is usually prohibitive. This sparsity of data has been recognized by the designers of the Sulfate Regional Experiment [3],

> "Existing data are not adequate to describe fully the chemical conversion from SO_2 (sulfur dioxide) to the sulfates and the removal processes of sulfur oxides. There is a great need for time-dependent three-dimensional measurements of many aerometric quantities to characterize the evolution and fate of the atmospheric SO_2."

It is precisely in this area that spacecraft observations, with their ability to provide synoptic data, could be most useful if they were able to provide the temporal sampling and spatial resolution which is required.

5.2.3 Temporal Sampling

The time scale specified for regional pollutant monitoring should be based on the time scales of the major factors which influence regional pollutant concentrations. These include:

- variations in mobile source emissions caused by the occurrence of "rush hours" in urban areas,
- variations in power plant or industrial emissions,
- diurnal and other variations in meteorological variables and,
- chemical and photochemical rates of reaction.

All four of the above factors have time scales which are less than 24 hours, indicating a need for observations more frequently than daily although a wide range of data-taking rates are useful [4]:

> "Temporal resolution needs in the troposphere vary widely and are for the most part poorly defined. For research purposes, intervals of from minutes to several tens of minutes can be important. At the other extreme, monitoring and control standards specify instantaneous peak readings through 1-hour and 24-hour averages and up to annual averages."

REFERENCES

1. _____, "Practical Applications of Space Systems, Supporting Paper 7, Environmental Quality." The Report of the Panel on Environmental Quality to the Space Applications Board of the Assembly of Engineering, National Research Council, National Academy of Sciences, Washington, D.C., 1975.

2. E. L. Keitz, E. J. Friedman and R. G. Eldridge, "The Capability of Remote Sensing for Regional Atmospheric Pollutant Studies," The MITRE Corporation, MTR-7267, January 1977.

3. G. M. Hidy, et. al., "Design of the Sulfate Regional Experiment (SURE), Volumes I-IV," Environmental Research Technology, Westlake Village, California, February 1976.

4. M. L. Wright, et. al., "A Preliminary Study of Air Pollution Measurement by Active Remote Sensing Techniques," Stanford Research Institute, NASA CR-132724, June 1975.

5. R. L. Myers and J. A. Reagen, "The Regional Air Monitoring System, St. Louis, Missouri, USA," International Conference on Environmental Sensing and Assessment, Las Vegas, Nevada, September 1975, The Institute of Electrical and Electronics Engineers, Inc., New York, 1976.

6. R. B. Evans, "Aerial Air Pollution Sensing Techniques." Proceedings Second Conference on Environmental Quality Sensors, National Environmental Research Center, Las Vegas, Nevada, October 1973.

7. _____, "Investigation of Rural Oxidant Levels as Related to Urban Hydrocarbon Control Strategies," prepared by the Research Triangle Institute for the U.S. Environmental Protection Agency, March 1975.

8. C. W. Spicer, et. al., "Final Data Report on the Transport of Oxidant Beyond Urban Areas," EPA Contract No. 68-02-2241, January 16, 1976.

9. R. T. H. Collis, "Regional Air Pollution Study: A Prospectus, Part III-Research Facility," Stanford Research Institute, Contract No. 68-02-0207, January 1972.

6.0 CONCLUSIONS AND RECOMMENDATIONS

The capabilities of the proposed instrument/orbit combinations have been made clear in earlier sections. Individual sites in the area of interest will be characterized by estimates whose uncertainty will be no smaller than 28 percent if the missions are of seven day duration (as currently proposed). Longer missions will result in proportionately smaller uncertainties, as described in Table 4-III.

It is also clear from the orbit traces that the one-day repeat cycle, which exhibits the minimum uncertainty, has the poorest coverage of the area of interest. Longer repeat cycles exhibit a denser coverage of the area but are characterized by higher uncertainties.

Data quality is also limited by instrument performance characteristics. Most important is the fact that no method currently exists for directly obtaining pollution data on the lowest altitudes of the atmosphere, the region which is most highly polluted. Other operating limits, as depicted in Section 2, result in overall performance capability which falls short of the requirements expressed for scientific or regulatory missions. Scientific needs require high data quality specific to the region of interest with reasonably complete spatial sampling. Regulatory uses require high data quality over long periods. These performance goals lie outside the range of capability of the proposed missions.

The instrument/orbit combinations do, however, hold the possibility for providing qualitative data on the movement of polluted

air masses. Under the conditions imposed by the sponsor on instrument selection and orbit characteristics, this qualitative data will be sufficient to inform the public of the long-range transport of polluted air, illustrate the general relationship between meteorology and air pollution and, possibly, identity major pollution sources. The results of the study also show that mission durations which greatly exceed the currently proposed seven day flight, will result in data quality which, while not being sufficient for scientific or regulatory purposes, may be adequate to provide a reliable picture of pollution levels.

The value of the data to the public will, of course, be a function of its accuracy and the fidelity with which it describes the region of interest. It is evident, then, that data analysis procedures which allow determination of pollution levels near the ground are greatly needed. The experiment as described in this report is arbitrarily limited by the fact that only nadir-viewing instruments are considered. The inclusion of some method of cross-track scanning would allow the selection of short repeat cycle orbits (which minimize uncertainty in the pollution estimates) but still provide good spatial coverage of the region of interest by scanning the field-of-view to the areas which the satellite does not fly directly over. This approach is not a complete solution to the spatial-temporal sampling problem, however, since the number of samples is still limited by the duration of the mission. Scanning

off the orbit track will reduce the number of observations of areas directly below the spacecraft in order to provide more complete spatial sampling between the orbit tracks. The most appropriate solution to limited sampling is increasing the duration of the mission, as is illustrated in Table 4-III.

APPENDIX A

ORBIT ANALYSIS PROCEDURES

A.0 ORBIT ANALYSIS

The following sections briefly describe the steps required to compute orbit parameters, orbit propagation and solar elevation and azimuth angles [1]. A glossary is included along with the logic used in computation of the orbit propagation.

A.1 Symbols

x1 = 66058.33128

x2 = 2π = 6.283185

x3 = 398601.2 = G•Me

x4 = 57.296 = degrees per radians

x5 = 0.9856473 = angular velocity of the Earth-sun line in degrees per day

G = gravitational constant = $6.67 \times 10^{-20} \quad \frac{Km^3}{Kg\ sec^2}$

Me = mass of the Earth = 5.983×10^{24} Kg

AO = unperturbed semi-major axis of orbit in km

E = eccentricity of orbit

I = inclination of orbit in degrees

TO = unperturbed periods, seconds

MO = unperturbed mean motion, radians/second

MI = mean motion, degrees/day, including perturbation due to first-order non-sphericity of the Earth

D1 = perigee rate, degrees/day

D2 = node rate, degrees/day

D3 = perigee step, degrees/mean anomaly step

D4 = node step, degrees/mean anomaly step

D5 = an intermediate step in the computations

D6 = daily synchronous orbit precession

D7 = yearly synchronous orbit precession

PO = an intermediate step in the computations

T1 = anomalistic period

T2 = nodal period

Q = repetition factor

Q1 = synchronous repetition factor

SO = unperturbed synchronous inclination

S = synchronous inclination

D = mean anomaly step

ℓ = argument of the orbit

R = longitude between successive ascending nodes

λ_o = initial longitude

α = solar elevation angle

ϕ = latitude

λ = longitude

β = solar azimuth

N = orbit number

δ = declination of the sun

ω = hour angle of the sun

n = number of days from vernal equinox.

A.2 Glossary [2]

anomalistic period - the time elapsing between successive passages of a satellite through its perigee

anomaly - the geocentric angle of a point along a satellite orbit as measured from perigee

argument - the geocentric angle of the point measured from ascending node in the orbital plane and in the direction of motion

azimuth of the sun - angular distance of the sun from north (east is positive)

declination - angle between the Earth-sun line and the equatorial plane

eccentricity - the ellipticity of an orbit

hour angle - angular distance of the sun from the meridian (or longitude) of the observer

inclination - the angle between the orbital plane of a satellite and the equatorial plane measured at the ascending node

mean anomaly - the geocentric angle which would be swept out by a satellite radius vector, since the last passage through perigee, if the satellite moved at uniform speed--it is directly proportional to the time since passage through perigee

nodal period - the time elapsing between successive passages of a satellite through its ascending node

node - intersection of the orbit track and the equatorial plane of the Earth

solar elevation - angular elevation of the sun above the horizon.

A.3 Equations

$$PO = [A0 \cdot (1 - E^2)]^2 \qquad (1)$$

$$T0 = x2 \cdot A0 \cdot \sqrt{A0/x3} \quad (2)$$

$$M0 = x2/T0 \quad (3)$$

$$M1 = M0 * \left[1 + \frac{x1 \cdot \sqrt{1 - E^2} \cdot (1 - 1.5 \sin^2 I)}{P0}\right] x4 \cdot 86400 \quad (4)$$

$$D1 = \frac{x1 \cdot M1 \cdot (2 - 2.5 \sin^2 I)}{P0} \quad (5)$$

$$D2 = -\frac{x1 \cdot M1 \cdot \cos I}{P0} \quad (6)$$

$$T1 = \frac{x2 \cdot 180 \cdot 86400}{M1 \cdot \pi} \quad (7)$$

$$T2 = \frac{x2 \cdot 180 \cdot 86400}{(M1 + D1) \cdot \pi} \quad (8)$$

$$S0 = \arccos\left[\frac{-A0^{1.5} \cdot P0 \cdot x5}{x1 \cdot \sqrt{x3} \cdot x4 \cdot 86400}\right] \quad (9)$$

$$S = \arccos\left[\frac{\cos S0}{1 + \frac{x1}{P0} \cdot \sqrt{1 - E^2} \cdot (1 - 1.5 \sin^2 S0)}\right] \quad (10)$$

$$D3 = \frac{x1 \cdot (2 - 2.5 \sin^2 I) \cdot D}{P0} \quad (11)$$

$$D4 = -\frac{x1 \cdot \cos I \cdot D}{P0} \quad (12)$$

$$D5 = M0 \cdot \left[1 + \frac{x1 \cdot \sqrt{1 - E^2} \cdot (1 - 1.5 \sin^2 S)}{P0}\right] \quad (13)$$

$$D6 = -\frac{x1 \cdot D5 \cdot \cos S \cdot x4 \cdot 86400}{P0} \quad (14)$$

$$D7 = D6 \cdot 365.2422 \quad (15)$$

$$Q = \frac{M1 + D1}{\frac{0.7292115061 \times 10^{-4} \cdot 180}{\pi} \cdot 86400 - D2} \quad (16)$$

$$Q1 = \frac{M1 + D1}{360} \quad \text{with M1 and D1 computed at inclination S.} \quad (17)$$

A.4 The Repetition Factor [3]

The longitudinal position of the ascending node moves an amount each orbit equal to

$$R = (\dot{\theta} - D2)\ \frac{T2}{86400} \quad \text{degrees of latitude} \tag{18}$$

where

$\dot{\theta}$ is the rotational velocity of the Earth relative to the stars (360.9856473 degrees per day).

The repetition factor Q, the number of orbits per day, is given by:

$$Q = 360/R \tag{19}$$

Q can be written as

$$Q = I + \frac{p}{n} = 360/R \tag{20}$$

where

p/n is in its lowest denominator form and I is an integer. After In+p orbits, the nodes will have moved

$$(In+p)R = n360 \tag{21}$$

degrees in longitude and will be back at the starting point (since an integer number of circuits of the Earth will have been completed, and n is the smallest integer which satisfies Equation 20). The number of days required for the orbit to repeat (a repeat cycle) can be found by noting that, since Q is the number of orbits per day,

$$nQ = In+p \text{ (orbits)} \tag{22}$$

so that the repeat cycle = n.

That is, n is the number of days required for repeat coverage of a particular longitude at the equator (and all other suborbital points on that orbit trace). Thus, any values of p and n represent an orbit with an n day repeat cycle. A special case exists if Q is an integer. Then, n = 1 and a one-day repeat period exists.

The numoer of orbits within the period of the repeat cycle dete.-mines the sequence in which regions are sampled.

Consider the descending node. If the westward displacement of the node per oribt is R degrees, then after an integral number of orbits, I, the node will have moved IR degrees. If an additional fractional orbit occurs each day (that is Q is an integer plus a fraction), then definition of the nodal movement per day becomes more complex since R can only be measured at the equator. If we define the nodal movement per day to be measured to the nearest integral orbit, then a Q with fraction $< 1/2$ will be rounded down to I orbits per day.

Thus, the nodal movement will be

$$\text{IR degrees per day for } \frac{p}{n} < 1/2 \quad . \tag{23}$$

If $p/n > 1/2$ then the orbits per day is rounded up to I+1 so that the nodal movement is

$$(I+1)R \text{ degrees per day for } \frac{p}{n} > 1/2 \quad . \tag{24}$$

Using this method, we see that if $p/n < 1/2$ for each successive day, the movement of the node will move toward the east (since a

fraction of an orbit is removed each day). If $p/n > 1/2$ the movement will be to the west.

The amount of longitudinal movement of the node is then equal to

$$-\frac{p}{n} R \quad \text{for} \quad \frac{p}{n} < 1/2 \tag{25}$$

and

$$(1 - \frac{p}{n})R \quad \text{for} \quad p/n > 1/2 \tag{26}$$

noting that the minus sign represents eastward movement.

A.5 Orbit Propagation

The propagation of the orbit in longitude and latitude is conveniently expressed in terms of the argument of the orbit, ℓ.

$$\Phi = \text{latitude} = \arcsin [\sin (180\text{-}I) \sin \ell] \tag{27}$$

$$\lambda = \text{longitude} = \lambda_o + \arctan [\cos (180\text{-}I) \tan \ell] \tag{28}$$

$$+ \ell/Q + \frac{N-nQ-1}{Q} \cdot 360 - 180 \cdot P$$

where

n is incremented by 1 each time N-1 exceeds Q

$P = 0$ for $\ell < 90$

$P = 1$ for $270 > \ell > 90$.

An additional correction must be made if λ exceeds 180°*:

if $\lambda < -180°$ then $\lambda = \lambda + 360°$

if $\lambda > 180°$ then $\lambda = \lambda - 360°$.

Generally, ℓ is restricted to range from 0 to 360 degrees. As a result, the orbit number, N, is increased by one each time ℓ reaches 360°.

*Note: Positive λ is measured westward from the Greenwich Meridian and negative λ is measured eastward.

The orbit propagation is defined by Equations 27 and 28 and the initial longitude of the ascending node, λ_o, of the orbit. Of course, λ_o changes from orbit to orbit by

$$\frac{360^\circ}{Q} \quad . \tag{29}$$

A.6 Solar Elevation Angle and Azimuth

The solar elevation angle, α, is a function of latitude, ϕ, declination of the sun, δ, and hour angle of the sun, ω.

The declination of the sun refers to its position relative to the Earth's equatorial plane and can be expressed as

$$\delta \cong 23.5 \sin 0.9856\ n \tag{30}$$

where

n = number of days from vernal equinox.

The hour angle of the sun is defined such that

ω = 0 at noon and equals 90° at 6 p.m.

The mathematical expression of the solar elevation angle is [4,5]

$$\sin \alpha = \sin \phi \sin \delta + \cos \phi \cos \delta \cos \omega \tag{31}$$

and the solar azimuth is given by

$$\sin \beta = - \frac{\cos \delta \sin \omega}{\cos \alpha} \quad .$$

This expression can be used with the formulae of the previous sections to compute the solar elevation angle along the orbit track.

The hour angle is given by

$$\omega = \omega_o + \lambda_o - \lambda + 1/Q \quad \frac{0.9856\ell}{360} + (N-1)\ (360.9856-D2) \qquad (32)$$

where

ω_o is the hour angle at the first equatorial crossing at the initial longitude λ_o. ω_o is usually taken to be 0 for non-synchronous orbits and, or course, equal to the appropriate hour angle for synchronous orbits.

The first term in brackets represents the movement of the sun during the time the satellite moves through ℓ degrees of argument ($0 \leq \ell \leq 360$) while the second term represents the movement of the sun relative to λ_o during (N-1) orbits.

If $\omega < -180°$ then $\omega = \omega + 180°$ (ω is positive west of Greenwich Meridian, negative east of Greenwich Meridian).

To convert to local sun time:

$$\text{if } \omega > 0 \quad t = \omega/15$$

$$\text{if } \omega < 0 \quad t = -\frac{(180+\omega)}{15}$$

(positive times are p.m. and negative times are a.m.).

A.7 Program Documentation

Computation of the latitude is straightforward and is described by Equation 27. The longitude computation is more complex due to the need to keep the range in the conventional limits of 0 to 180 west of the Greenwich Meridian and 0 to -180 east of the Greenwich Meridian, as well as noting the longitudinal movement from orbit to orbit and day-to-day.

Figure A-1 illustrates the flow and decision process associated with the calculation of latitude and longitude.

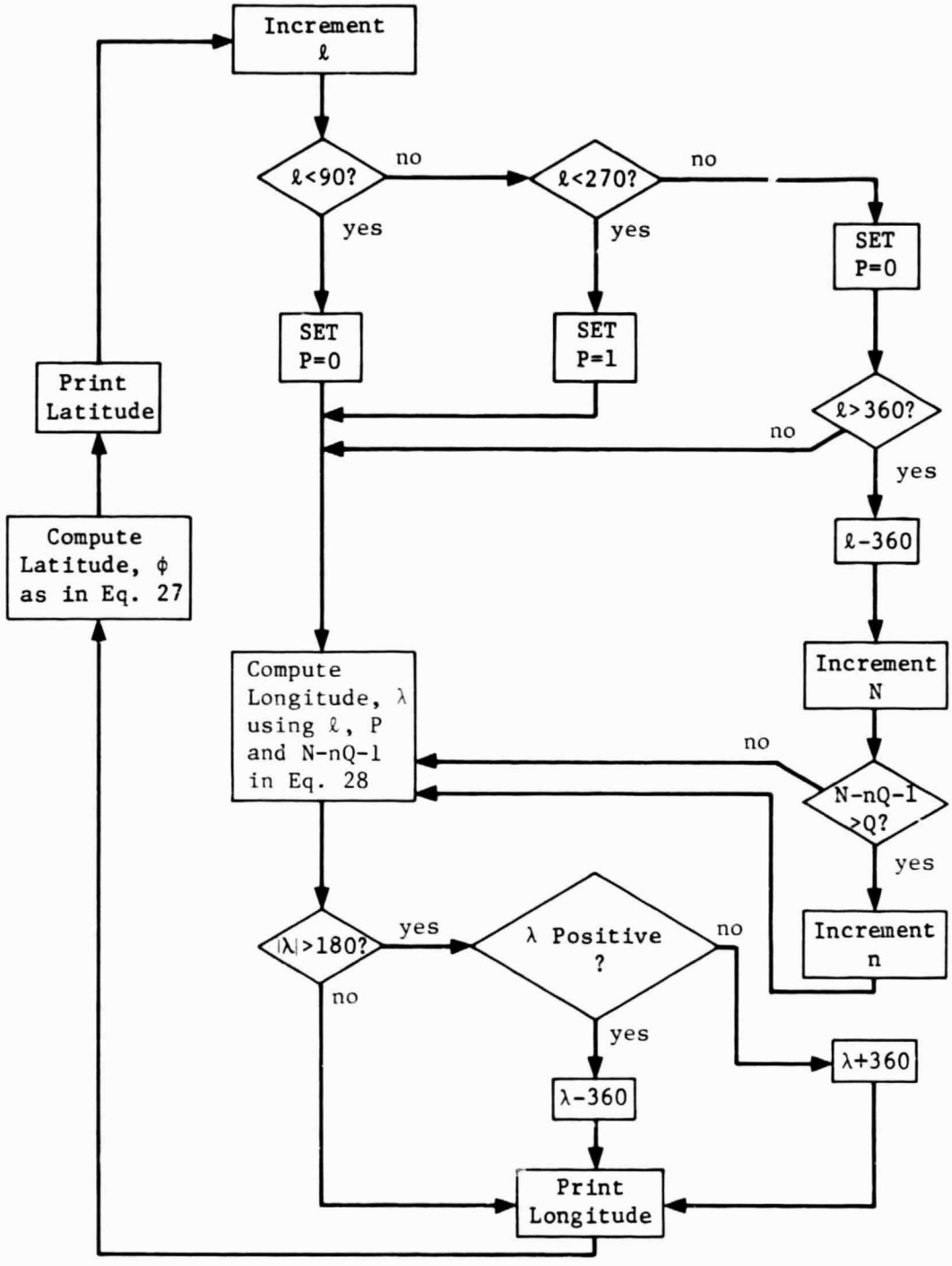

FIGURE A-1
FLOW DIAGRAM FOR COMPUTATION OF LATITUDE AND LONGITUDE

REFERENCES

1. D.R. Brooks, "An Introduction to Orbit Dynamics and Its Application to Satellite-Based Earth Monitoring Missions." NASA RP-1009, October 1977.

2. W.K. Widger, Jr. "Orbits, Altitudes, Viewing Geometry Coverage and Resolution Pertinent to Satellite Observations of the Earth and its Atmosphere," in Proceedings of the Fourth Symposium on Remote Sensing of the Environment, Ann Arbor, Michigan.

3. R.B. Gerding, et al. "Coastal-Zone Oceanographic Requirements for Earth Observatory Satellites A & B," NASA CR-111816, February 1971.

4. M.I. Budyko, Climate and Life, Academic Press, New York, 1974.

5. R.J. List, Smithsonian Meteorological Tables, Sixth Edition, Smithsonian Institution Press, Washington, D.C., 1949.

APPENDIX B

INCIDENCE AND DURATION OF CLOUDINESS IN WASHINGTON, D.C.

B.0 INTRODUCTION

The basic purpose of this appendix is to analyze the frequency of occurrence and duration of cloudy versus clear periods at a selected location (Washington, D.C.). This location is assumed to be representative of the Eastern U.S. and can, therefore, be used as a measure of the frequency with which clouds inhibit operation of infrared remote sensors. The average cloudiness statistic, which is calculated from measurements at National Weather Service Stations, provides no information on these statistics.

This appendix is presented in two main sections. In the first, the clear versus cloudiness statistics which were obtained from the National Climatic Center are described. In the second section, the ten year annual average data for Washington, D.C., are analyzed to give an example of how the data could be used and what typical results indicate.

B.1 Cloud Patterns

In the temperate climatic zone which is typical of most of the United States, clear and cloudy periods can be correlated with the passage of high and low pressure cells and their associated frontal systems. This produces cycles of clear and cloudy days, the duration of which is somewhat correlated with the speed of movement of the fronts and pressure cells. Slower movement produces longer periods

of clear and cloudy days and long stagnant periods are usually associated with quasi-stationary systems.

This characteristic of temperate zone weather produces a cyclical pattern of clear and cloudy days which typically consists of one to three cloudy days followed by a similar number of clear days. Analysis of data showing the frequency of occurrence and the duration of these cloudy and clear periods is necessary as an input to evaluating the sampling gaps which may occur.

A complicating factor is introduced when one recognizes that partly cloudy conditions do occur and, in fact, are probably the most usual case over much of the United States. Thus, the analysis would consider a selected number of categories of partly cloudy conditions in addition to completely clear and completely cloudy cases. The other factor which could be considered is that clear, cloudy or partly cloudy conditions do not occur in convenient one day increments but may change from hour to hour or even more frequently in some cases. At this level of complexity, analysis of the actual hour by hour reports of cloud amounts at the location of interest would be necessary.

In order to achieve the basic purpose of this appendix, i.e., demonstrating the statistics of the cloudiness data, it was decided to obtain the necessary data to perform an analysis as discussed below. The basic statistic of interest would be the frequency of occurrence of cloudy periods of n days duration which are preceded by

a clear period of m days duration. The National Climatic Center was contacted to provide such data. Since the data are nonstandard, it was necessary to prepare a specific computer program which would generate the data from standard observations. This program had the following specifications:

1. Based on standard National Weather Service hourly (during daylight) observations of total cloud cover, each day at each station of interest was categorized as either clear or cloudy by determining the arithmetic mean of the total cloud cover for all hours from sunrise to sunset. Days with five-tenths or less mean total cloud cover were categorized as clear and days with six-tenths or more total cloud cover were categorized as cloudy. The simple assumption is therefore made that the amount of sunshine available during periods when total cloud cover is between six-tenths and nine-tenths is offset by the amount of sunshine which is lost during periods when total cloud is between one-tenth and five-tenths.
2. Cycles of clear and cloudy days were determined and counts were made of the number of occurrences n cloudy days preceded by m clear days. n and m were presented in eleven categories each (1 to 10 and >10).
3. Observations for the ten-year period from 1965 through 1974 were analyzed.

The results were presented by individual season and annually for each of the ten years and for the total of the ten-year period. Seasons were defined as:

Winter - December to February
Spring - March to May
Summer - June to August
Fall - September to November

Those episodes which extended over two seasons or two years were arbitrarily categorized into the time slot corresponding to the first clear day of each clear/cloudy cycle.

A sample of this data is shown in Table B-I which presents the average values of cloudiness for Washington, D.C. for the period 1965 to 1974. This particular data set was used in the analysis presented in Section 4.

The table illustrates that the most probable pattern of cloudiness is one in which a clear day is followed by a cloudy day. Also highly likely is the case that a clear day is followed by two cloudy days. Extended periods of cloudy or clear conditions become less likely as the time interval is extended. It is also interesting to note that the total number of cloudy days in the period of study was 2157 while the number of clear days was 1462.

Inspection of the totals for cloudy periods illustrates that of the 721 periods which occurred (of varying durations) over 70 percent were of three days or less.

TABLE B-I

FREQUENCY OF OCCURRENCE OF n CLOUDY DAYS WHICH ARE PRECEDED BY m CLEAR DAYS; WASHINGTON, D.C., 1965-1974

DURATION OF CLEAR PERIOD (DAYS)	DURATION OF CLOUDY PERIOD (DAYS)											
	1	2	3	4	5	6	7	8	9	10	>10	TOTAL
1	118	90	53	36	20	18	9	11	5	4	12	376
2	40	49	33	14	9	3	6	6	2	1	2	165
3	46	16	18	4	5	4	4	1		1	4	103
4	10	11	3		2		1		1	1		29
5	6	7	2		2	1	1		1			20
6	6	5	1				1					13
7	3	2	2									7
8	2											2
9			1	2								3
10			1									1
>10		1			1							2
TOTAL	231	181	114	56	39	26	22	18	9	7	18	721

TOTAL NUMBER OF DAYS WITH VALID DATA: 3619 (99.1% of total possible days).